EUROPEAN ORGANIZATION FOR NUCLEAR RESEARCH (CERN)
FERMILAB-PUB-11-747-CMS

CERN-PH-EP/2011-171
2011/11/01

CMS-QCD-10-035

Measurement of the Production Cross Section for Pairs of Isolated Photons in pp collisions at $\sqrt{s} = 7\,\text{TeV}$

The CMS Collaboration*

arXiv:1110.6461v1 [hep-ex] 28 Oct 2011

Abstract

The integrated and differential cross sections for the production of pairs of isolated photons is measured in proton-proton collisions at a centre-of-mass energy of 7 TeV with the CMS detector at the LHC. A data sample corresponding to an integrated luminosity of 36 pb^{-1} is analysed. A next-to-leading-order perturbative QCD calculation is compared to the measurements. A discrepancy is observed for regions of the phase space where the two photons have an azimuthal angle difference $\Delta\varphi \lesssim 2.8$.

Submitted to the Journal of High Energy Physics

*See Appendix A for the list of collaboration members

Operated by Fermi Research Alliance, LLC under Contract No. De-AC02-07CH11359 with the United States Department of Energy.

1 Introduction

The production of energetic photon pairs in hadronic collisions is a valuable testing ground of perturbative quantum chromodynamics (pQCD). The emission of a pair of photons from hard parton-parton scattering constitutes a particularly clean test of perturbation theory in the collinear factorisation [1, 2] and k_{T} factorisation [3] approaches, as well as soft-gluon logarithmic resummation techniques [4]. A comprehensive understanding of photon pair production is also important as it represents a major background in certain searches for rare or exotic processes, such as the production of a light Higgs boson, extra-dimension gravitons, and some supersymmetric states.

This paper presents a measurement of the production cross section for isolated photon pairs in proton-proton collisions at a centre-of-mass energy of 7 TeV, using the Compact Muon Solenoid (CMS) detector at the Large Hadron Collider (LHC). Isolated photons produced in the hard scattering of quarks and gluons are henceforth referred to as *signal photons* and the remaining photons as *background photons*. A pair of signal photons will be referred to as a diphoton. The data sample was collected in 2010 and corresponds to an integrated luminosity of 36.0 pb^{-1}. Recent diphoton cross-section measurements have been performed by the D0 [5] and CDF [6, 7] Collaborations in proton-antiproton collisions at $\sqrt{s} = 1.96$ TeV, and by the ATLAS Collaboration at the LHC [8].

The CMS detector consists of a silicon pixel and strip tracker surrounded by a crystal electromagnetic calorimeter (ECAL) and a brass/scintillator sampling hadron calorimeter (HCAL), all in an axial 3.8 T magnetic field provided by a superconducting solenoid of 6 m internal diameter. The muon system is composed of gas-ionization detectors embedded in the steel return yoke of the magnet. In addition to the barrel and endcap detectors, CMS has an extensive forward calorimetry system. A more detailed description of CMS can be found elsewhere [9].

In the CMS coordinate system, θ and φ respectively designate the polar angle with respect to the counterclockwise beam direction, and the azimuthal angle, expressed in radians throughout this paper. The pseudorapidity is defined as $\eta = -\ln\left[\tan\frac{\theta}{2}\right]$.

Distance in the (η, φ) plane is defined as $R = \sqrt{(\Delta\eta)^2 + (\Delta\varphi)^2}$. The transverse energy E_{T} of a particle is defined as $E_{\mathrm{T}} = E\sin\theta$, where E is the energy of the particle, and the transverse momentum is $p_T = p\sin\theta$. The rapidity is defined as $y = \frac{1}{2}\ln\left[\frac{E+p_z}{E-p_z}\right]$, with p_z being the longitudinal momentum with respect to the beam axis.

The electromagnetic calorimeter, which plays a major role in this measurement, consists of nearly 76 000 lead tungstate crystals. It is divided into a central part (barrel) covering the region $|\eta| < 1.48$ and forward parts (endcaps) extending the coverage up to $|\eta| < 3$ for a particle originating from the nominal interaction point. The crystals are arranged in a projective geometry with a granularity of 0.0174 in both the η and φ directions in the barrel, and increasing with η from 0.021 to 0.050 in the endcaps. A preshower detector, consisting of two planes of silicon sensors interleaved with 3 radiation lengths of lead, is placed in front of the endcaps to cover the pseudorapidity region $1.65 < |\eta| < 2.6$.

The differential cross section is measured as a function of variables that are particularly relevant in searches for rare processes or to characterise QCD interactions (e.g. [2]):

- the diphoton invariant mass, $m_{\gamma\gamma}$;
- the azimuthal angle between the two photons, $\Delta\varphi_{\gamma\gamma}$;
- the photon pair transverse momentum, $p_{T,\gamma\gamma} = \sqrt{{p_{T,\gamma_1}}^2 + {p_{T,\gamma_2}}^2 + 2\,p_{T,\gamma_1}p_{T,\gamma_2}\cos\Delta\varphi_{\gamma\gamma}}$,

where p_{T,γ_1} and p_{T,γ_2} are the magnitudes of the transverse momenta of the two photons;

- $|\cos\theta^*| = |\tanh\frac{\Delta y_{\gamma\gamma}}{2}|$, with $\Delta y_{\gamma\gamma}$ being the difference between the two photon rapidities. At lowest order in QCD, θ^* is the center-of-mass scattering angle for the $q\bar{q} \to \gamma\gamma$ and $gg \to \gamma\gamma$ processes.

The event selection requires at least one isolated photon with $E_T > 23$ GeV and a second isolated photon with $E_T > 20$ GeV, separated by $R > 0.45$. The measurements are performed in two pseudorapidity regions, one with $|\eta| < 1.44$, and the other defined by the tracker acceptance $|\eta| < 2.5$, but excluding the transition region between the barrel and endcap calorimeters, $1.44 < |\eta| < 1.57$. For convenience the widest η range without the transition will be referred to as $|\eta| < 2.5$ throughout the paper.

The asymmetric thresholds on the photon transverse momenta avoid the infrared sensitivity affecting the fixed-order calculations [10, 11] and simplify the comparison of the measurements with the theoretical predictions.

All simulation results are based on the PYTHIA 6.4.22 [12] event generator, with the Z2 tune, the CTEQ6L parton distribution functions (PDFs) [13], and a GEANT4 [14] modelling of the detector. The Z2 tune is identical to the Z1 tune described in [15] except that Z2 uses the CTEQ6L PDFs while Z1 uses CTEQ5L [16]. At the generator level, a prompt photon is considered as signal if the sum of the generated transverse momenta of all the particles within a cone $R < 0.4$ around the photon direction is less than 5 GeV.

Event selection and background discrimination are presented in Sections 2 and 3. The determination of the signal yield and the measurement of the cross section are described in Sections 4 and 5. Systematic uncertainties are detailed in Section 6. Results are discussed in Section 8 and compared with the theoretical predictions introduced in Section 7.

2 Event Selection

Photon candidates are reconstructed by clustering the energy deposited in the ECAL [17, 18] crystals. CMS is equipped with a versatile trigger to adapt to the steady increase in the LHC instantaneous luminosity. In this measurement, three trigger settings were used for three successive data-taking periods. They require two photon candidates, with a threshold of either 15 GeV or 17 GeV on the transverse energy. For the last period, with the highest instantaneous luminosity, a weak isolation requirement is applied on one of the two photon candidates. For the three periods, the trigger efficiency for events passing the analysis selections described in the following paragraphs is estimated from simulated events to be greater than 99.9%. The offline event selection requires one photon candidate with $E_T > 23$ GeV and a second photon candidate with $E_T > 20$ GeV, each within the fiducial region defined in the introduction. The candidates are required to be separated by $R > 0.45$ to avoid energy deposits related to one candidate overlapping with the isolation region of another candidate.

Photon identification criteria requiring the deposits in the calorimeters to be consistent with an electromagnetic shower are applied to the two candidates. The criteria are based on the spread along η of the energy clustered in the ECAL, henceforth referred to as $\sigma_{\eta\eta}$, and on the ratio H/E of the energies measured in the HCAL and ECAL (*loose selections* of Ref. [18]).

The photon candidates are required to be isolated. The sum of the transverse momenta of charged particles measured by the tracker and the sum of the transverse energy deposits in the HCAL, both defined within a cone of radius $R = 0.4$ around the photon direction, must

each be less than 2 GeV in the barrel and 4 GeV in the endcaps. HCAL deposits in a cone of radius $R = 0.15$ are excluded from the sum, as well as tracks in a cone of radius $R = 0.04$ and within a strip of $\Delta\eta = 0.03$ along the φ direction, which can potentially contain tracks of an electron-positron pair from the conversion of a photon in the tracker material. The sum of the transverse energy deposited in the ECAL in a cone of radius $R = 0.3$ is required to be less than 20% of the photon transverse energy, in order to be consistent with the online trigger requirements. Excluded from the sum is the energy deposited within a cone whose radius corresponds to 3.5 crystals along η and within a 5-crystal-wide strip extending along the φ direction. In addition, we require that no charged particle with the following properties impinge on the ECAL within a cone of radius $R = 0.4$: transverse momentum $p_{\mathrm{T}} > 3$ GeV, impact parameters with respect to the primary vertex in the transverse and longitudinal planes of less than 1 mm and 2 mm, respectively, and one associated hit in the innermost layer of the pixel detector. Tracks corresponding to such particles are henceforth called *impinging tracks*. The electron contamination is further reduced by imposing an additional veto on the presence of hits in the layers of the pixel detector along the direction of the photon candidate.

3 Signal and Background Discrimination

The photon candidates in the selected event sample are designated as signal photons, background photons from hadron decays (most of which are misidentified pairs of collinear photons coming from neutral meson decays), or misidentified electrons. The background to diphoton pair events is thus made up of photon+jet and multijet events, with respectively one and two background photons from neutral hadron decays, and Drell–Yan events, with two misidentified electrons.

The contamination from Drell–Yan events is estimated from simulation using the next-to-leading-order (NLO) POWHEG generator [19–21], which agrees well with our own Drell–Yan measurement [22]. The diphoton cross-section measurement is corrected for this contamination, which amounts to about 12% in the diphoton mass range 80–100 GeV around the Z peak. This procedure has a negligible impact on the systematic uncertainties.

Background photons from photon+jet and multijet events are produced in jets alongside other particles, which tend to widen the deposits in the ECAL. An isolation variable $\mathcal{I}$ based on the energy in the ECAL is used to statistically estimate the fraction of diphoton events among the selected candidates. This variable is constructed to minimise the dependence on the energy deposited by minimum-ionising particles (MIPs) such that its distribution for the background can be obtained from the data by means of the impinging-track method described below. It is defined as the sum of the transverse energy of the ECAL deposits with $E_{\mathrm{T}} > 300$ MeV (MIP veto), within a hollow cone centred on the photon impact point, with an inner radius of 3.5 crystal widths and an outer radius of $R = 0.4$. Deposits assigned to the photon itself or falling within a 5-crystal-wide strip extending along φ and centred on the photon impact point are removed. Thus, deposits from photons converting into electron-positron pairs in the tracker material and spread along the φ direction do not contribute to the value of $\mathcal{I}$. The variable $\mathcal{I}$ differs from the ECAL isolation used in the selection described in Section 2.

As the distribution of $\mathcal{I}$ is different for signal photons and background photons, this variable can be used in a maximum-likelihood fit to extract the number of signal events in the entire selected sample. Figure 1 shows the probability density function of $\mathcal{I}$, which was extracted from data with the methods described below.

Contributions to the value of $\mathcal{I}$ for signal photons come from pileup (multiple proton-proton

collisions in the same bunch crossing) and underlying-event activity (multiple parton interaction and beam remnants from the same proton-proton collision). Since these contributions are independent of φ, the ECAL isolation probability density function $f(\mathcal{I})$ is estimated from *random cones* using events with at least one isolated photon candidate. The value of $\mathcal{I}$ is calculated in a cone of radius $R = 0.4$ around an axis at the same value of η as the photon candidate and at a random value of φ within a window of width $\pi/2$ centred on the axis perpendicular to the photon direction, with the same exclusions applied to photon signals. The cone is required not to include any photon or electron candidates or jets. The function $f(\mathcal{I})$ for signal photons is validated with two additional independent methods. Both methods exploit e^+ and e^- from Z and W boson decays that do not radiate significantly in the tracker material. The e^+ and e^- are selected with a constraint imposed on the fraction of bremsstrahlung energy emitted from the interaction in the tracker material. Such electrons and positrons leave ECAL energy deposits consistent with those of photons, and have a similar probability density function for $\mathcal{I}$. The $Z \to e^+e^-$ events are selected with stringent requirements on the identification criteria of the lepton pair and on its invariant mass, and the $f(\mathcal{I})$ distribution is obtained directly from both leptons. In $W \to e\nu_e$ events, $f(\mathcal{I})$ is obtained by exploiting the *sPlot* technique [23]. The missing transverse energy projected along the lepton axis is used to estimate the probability of an event to be signal ($W \to e\nu_e$) or background ($Z \to e^+e^-$, $W \to \tau\nu_\tau$, $\gamma +$ jet(s), and QCD multijet processes). The value of $\mathcal{I}$ for the selected candidates is weighted accordingly to estimate the distribution of $\mathcal{I}$. The uncertainty on $f(\mathcal{I})$ is taken as the maximum difference between the distributions extracted from random cones and from electrons in Z and W events. In simulated events, the difference between $f(\mathcal{I})$ for signal photons and for random cones is smaller than the uncertainty determined from data.

For background photons, $f(\mathcal{I})$ is extracted from a sample with less than 0.1% of signal-photon contamination. The sample is obtained by selecting photon candidates with one and only one impinging track. A cone of radius $R = 0.05$ around the track is excluded from the isolation area to avoid counting the energy deposited by the charged particle. The isolation variable $\mathcal{I}$ is then rescaled to take into account this additional exclusion. To validate this method, the $\mathcal{I}$ distribution is also extracted from a sample of events with two impinging tracks, one of the two being excluded in the computation of $\mathcal{I}$. The latter distribution is compared to that obtained with the one-impinging-track sample, using the normal definition of $\mathcal{I}$, i.e., including the energy deposits in the vicinity of the track. The agreement is within one standard deviation for the entire range of the $\mathcal{I}$ distribution, and the difference is taken as a systematic uncertainty on $f(\mathcal{I})$ for background photons.

The distributions $f(\mathcal{I})$ show a moderate dependence on η and on the pileup conditions, the latter being quantified by the number n_{vtx} of primary vertices in the events (2.4 on average). The background distribution $f(\mathcal{I})$ also depends on the transverse energy E_{T} of the candidate. Therefore, events in the sample used for the extraction of $f(\mathcal{I})$ are weighted to reproduce the distributions of η, n_{vtx}, and E_{T} of the diphoton sample used for the cross section measurement. The effect of using the distributions from the diphoton sample to correct the biases in the background and signal shapes used in the maximum-likelihood fit is addressed in the systematic uncertainty section, Section 6.

4 Signal Yield Determination

The number of diphoton events is obtained from a binned maximum-likelihood fit to the distributions of the ECAL isolation variables of the two photons, $\mathcal{I}_1$ and $\mathcal{I}_2$, whose ordering is chosen randomly. Events are separated into three types: signal events ($\gamma\gamma$) if both photons

are signal photons, background events with a signal photon and a background photon, and background events with two background photons.

The likelihood function $\mathcal{L}$ that is maximised in the fit is

$$\mathcal{L} = \frac{e^{-N^{\text{tot}}}}{N!} \prod_{i=1}^{N} \sum_{t=1}^{3} N_t f_t(\mathcal{I}_1^i, \mathcal{I}_2^i) \,, \tag{1}$$

where N is the number of selected events, N_t is the number of events estimated in the fit for event type t, N^{tot} is their sum, and $f_t(\mathcal{I}_1, \mathcal{I}_2)$ is the probability for the ECAL isolation variables of the two photons to have values $\mathcal{I}_1$ and $\mathcal{I}_2$ for a given event type t.

The probability density functions $f_t(\mathcal{I}_1^i, \mathcal{I}_2^i)$ for the three event types are obtained by multiplying the probability density functions $f(\mathcal{I})$ for single-photon candidates, assuming the two statistical variables $\mathcal{I}_1$ and $\mathcal{I}_2$ to be independent. Correlations between these two variables have been checked with simulation and are negligible.

A total of 5977 events pass the selection criteria described in Section 2. These events are divided into three subsamples depending on whether both photons are in the barrel (2191 events), one is in the barrel and the other in the endcaps (2527 events), or both are in the endcaps (1259 events). The fit is performed separately for each of the three subsamples and each bin of the four observables. An example of the fit for one bin of the $m_{\gamma\gamma}$ spectrum is shown in Fig. 2 for events with both photons in the barrel ($|\eta| < 1.44$).

The maximum-likelihood method is known to be biased for samples with small numbers of events [24]. This bias is estimated with Monte Carlo pseudo-experiments and the fit results are corrected for it. It is less than 10% of the statistical uncertainty for 80% of the fits and never exceeds half the statistical uncertainty.

5 Cross-Section Measurement

The differential diphoton cross-section measurement $d\sigma/dX$, for the variable X in the interval X_i, is

$$\frac{d\sigma}{dX}(X_i) = \frac{N_{\gamma\gamma}^{\text{U}}(X_i)}{\mathcal{L}\Delta X_i \mathcal{C}(X_i)} \,, \tag{2}$$

where $N_{\gamma\gamma}^{\text{U}}$ is the number of signal events obtained from the fit, unfolded for the detector resolution and corrected for the Drell–Yan contamination; $\mathcal{L}$ is the integrated luminosity, ΔX_i is the interval width; $\mathcal{C}$ is a correction factor for the effects of the detector resolution on the acceptance and on the efficiencies of photon reconstruction and identification.

The number of signal events is unfolded [25] for the detector resolution by inverting a response matrix T for each of the observables $m_{\gamma\gamma}$, $p_{T,\gamma\gamma}$, $\Delta\varphi_{\gamma\gamma}$, and $|\cos\theta^*|$, obtained from simulated events passing the selection requirements. The matrix elements T^{ik} are the probabilities of a selected event with the generated value of X in bin X_k to be reconstructed with a value of X in bin X_i. For a given interval X_k, the number of events after unfolding is related to the observed numbers of events in the different intervals X_i by $N_{\gamma\gamma}^{\text{U}}(X_k) = \left(T^{-1}\right)^{ki} N_{\gamma\gamma}(X_i)$. Here, $N_{\gamma\gamma}(X_i)$ is the signal yield corrected for the Drell–Yan contamination, as described in Section 3. Given the excellent energy resolution of the ECAL and the bin sizes, the matrix T is nearly diagonal, and thus no regularisation is applied in the unfolding procedure.

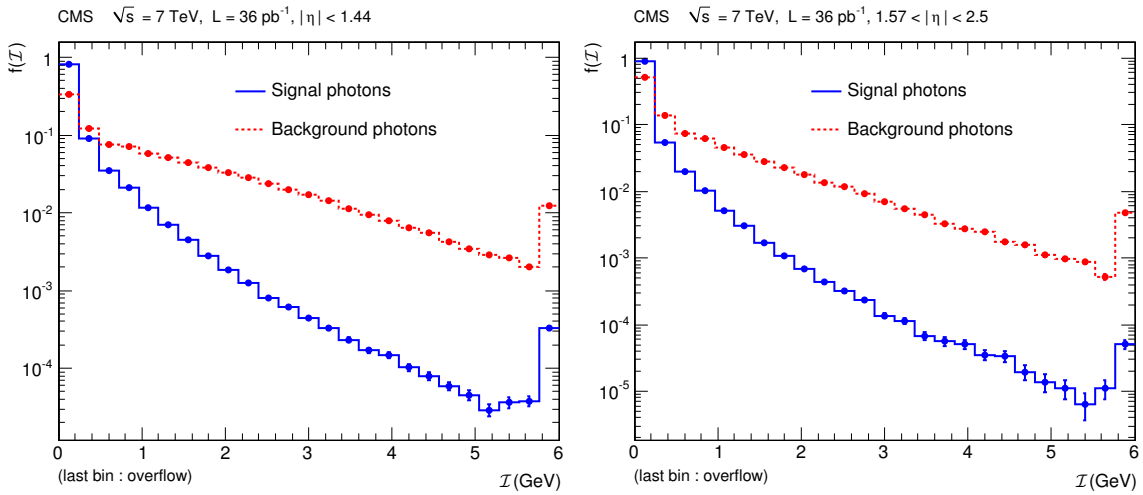

Figure 1: Probability density functions of the ECAL isolation variable $\mathcal{I}$ for signal photons (solid blue) and background photons (dashed red) in the barrel (left) and in the endcap regions (right).

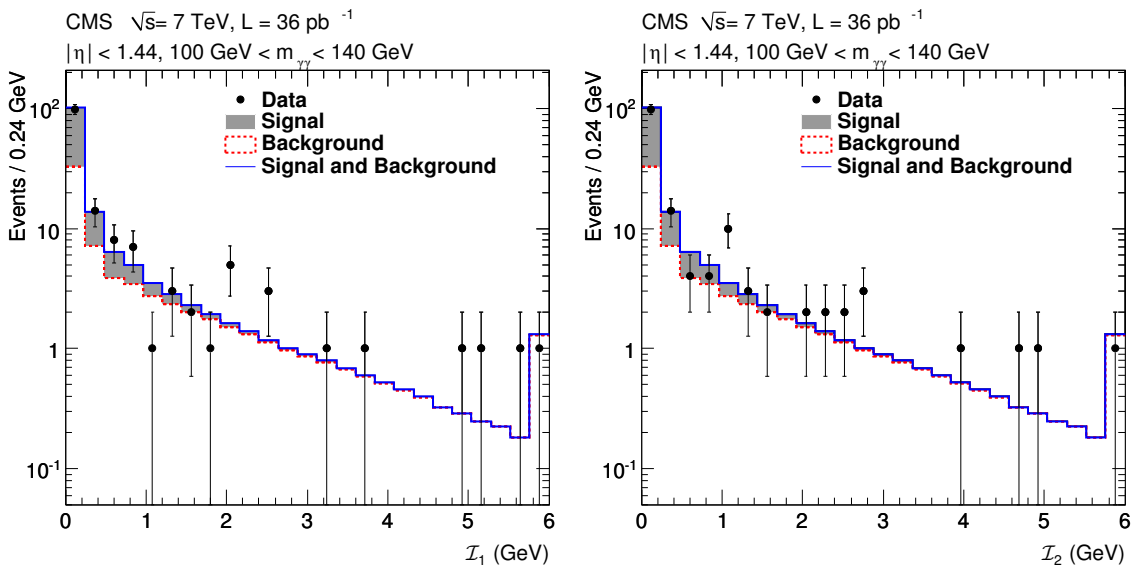

Figure 2: Fit to the photon ECAL isolation $(\mathcal{I}_1, \mathcal{I}_2)$ in the bin $100 < m_{\gamma\gamma} < 140$ GeV for photons with $|\eta| < 1.44$. The distribution of the isolation variable $\mathcal{I}_1$ of one photon candidate, arbitrarily chosen as the "first photon" and denoted with subscript "1", is displayed in the left figure, together with the fit result, integrated over $\mathcal{I}_2$; the shaded region shows the signal distribution, the dashed line represents the background contribution, while the solid line is the sum of the signal and background contributions. The same distributions for the second photon candidate are shown in the right figure. In this mass bin, the number of signal events is 72 ± 14, out of the total number of 161 selected candidates.

The correction factor $\mathcal{C}(X_i)$ is defined as

$$\mathcal{C}(X_i) = \frac{N^{\text{sim}}_{\text{reco}}(X_i)}{N^{\text{sim}}_{\text{gen}}(X_i)} \frac{\varepsilon^{\text{data}}}{\varepsilon^{\text{sim}}}, \tag{3}$$

where

$N^{\textbf{sim}}_{\textbf{reco}}(X_i)$ is the number of simulated events passing all the selection criteria, with generated values of X within the interval X_i;

$N^{\textbf{sim}}_{\textbf{gen}}(X_i)$ is the number of simulated events within the acceptance defined at the generator level (Section 1), with generated values of X within the interval X_i;

$\varepsilon^{\textbf{data}}$ is the efficiency of the photon identification criteria measured from data;

$\varepsilon^{\textbf{sim}}$ is the efficiency of the photon identification criteria obtained from simulated events using the same technique as for $\varepsilon^{\text{data}}$.

The efficiencies $\varepsilon^{\text{data}}$ and ε^{sim} to observe a diphoton candidate are taken as the square of the efficiencies to observe a single photon.

The efficiency for the requirements on isolation, $\sigma_{\eta\eta}$, and H/E is estimated with a "tag-and-probe" method [26] applied to a $\text{Z} \to \text{e}^+\text{e}^-$ sample selected from the full 2010 dataset. One lepton, the tag, is selected with tight reconstruction and identification criteria [27], while the other, the probe, is selected by requiring a constraint on the invariant mass of the lepton pair. The probes constitute a sample of unbiased electrons and positrons. The same constraint as discussed in Section 3 is applied on the fraction of bremsstrahlung energy emitted by the e^+ and e^- interacting in the tracker material. This requirement ensures that the electromagnetic deposits of these electrons and positrons are consistent with those of a photon shower. The efficiency is computed by applying the requirements on isolation, $\sigma_{\eta\eta}$, and H/E to this sample, and then measuring the fraction of probes passing the selection.

The efficiency for the requirement to have no impinging tracks within the isolation cone is estimated from data, from a control sample built using a *random-cone* technique on events with a single photon selected according to the identification criteria described above. The random-cone definition is that introduced in Section 3 for the extraction of $f(\mathcal{I})$. Particles within the random cone hence come mainly from pileup and the underlying event. Quantities such as the number of impinging tracks or energy deposits in the isolation area are therefore assumed to have the same distributions as for isolated photons. The efficiency of the requirement to have no impinging track within the isolation cone is given by the ratio of the number of random cones passing this criterion to the total number of random cones. The efficiency of the veto on pixel hits is obtained from simulation. It is included in the $N^{\text{sim}}_{\text{reco}}/N^{\text{sim}}_{\text{gen}}$ term of Eqn. (3).

The correction factor $\mathcal{C}$ is $(80.8 \pm 1.9)\%$ for the integrated cross section in the region $|\eta| < 1.44$, and $(76.2 \pm 3.3)\%$ in the region $|\eta| < 2.5$.

6 Systematic Uncertainties

The systematic uncertainty on the reconstructed photon four-momenta is dominated by the ECAL energy scale, known to 0.6% in the barrel and 1.5% in the endcaps [28]. The energy scale affects the value of the acceptance and induces bin-to-bin migrations in the differential cross

sections. The effect on the acceptance is relevant only in kinematic regions near the photon p_T thresholds and results in an uncertainty of 40% in the most affected region, the lowest values of $m_{\gamma\gamma}$. The uncertainty from the bin-to-bin migration is about 1%.

The systematic uncertainty on the measured photon identification efficiency ($\varepsilon^{\text{data}}$ in Eqn. (3)) is estimated by applying the tag-and-probe and random-cone methods on simulated events. The difference between the efficiency value obtained with these methods and that given by the fraction of simulated events passing the identification criteria is taken as the systematic uncertainty. The uncertainty from the acceptance and efficiency correction factor $\mathcal{C}$ is taken as the quadratic sum of the statistical uncertainties on the different factors of Eqn. (3) and the systematic uncertainty mentioned above. The systematic and statistical uncertainties on $\varepsilon^{\text{data}}$ total 1.9% for diphotons in the barrel and 3.3% for all diphotons.

The systematic uncertainties on the signal and background isolation probability distributions $f(\mathcal{I})$ are estimated with Monte Carlo pseudo-experiments in which $f(\mathcal{I})$ is varied. The variations correspond to the differences between the shapes of the nominal and validation distributions observed in the validation of the random-cone and impinging-track methods (Section 3). In the first bin of the probability density functions, they are of the order of ± 0.01 for the signal, and range from ± 0.03 to ± 0.05 for the background. The uncertainty on $f(\mathcal{I})$ from its dependence on the distribution of photon transverse energy E_T, photon pseudorapidity η, and number of vertices n_{vtx} is estimated from the change in $f(\mathcal{I})$ when using the E_T, η, and n_{vtx} distributions from the diphoton simulation instead of those from the diphoton event candidates in data. This contribution to the uncertainty is negligible. The overall systematic uncertainty from the $f(\mathcal{I})$ distributions on the integrated cross section is about 8%, and varies from 4 to 27% on the differential cross sections, depending on the bin and the subsample.

A 4% uncertainty is assigned to the integrated luminosity [29]. The various contributions to the systematic uncertainties are summarised in Table 1.

Table 1: Contributions to the systematic uncertainties on the measured differential cross sections for two pseudorapidity ranges. The uncertainties are computed for each bin of Figs. 3 to 10. The values listed below are averages.

Uncertainty source	$\lvert\eta\rvert < 1.44$	$\lvert\eta\rvert < 2.5$
Energy scale on acceptance	1.5%	2%
Energy scale on bin-to-bin migration	1%	1.5%
Signal and background distributions for $f(\mathcal{I})$	7%	9%
Acceptance and efficiency correction factor $\mathcal{C}$	2%	3%
Luminosity	4%	4%
Total	8%	11%

7 Theoretical Predictions

This section introduces the theoretical calculations whose predictions are compared to the experimental data in Section 8. The leading contributions to the production of pairs of prompt

photons in pp collisions are the quark-antiquark annihilation ($q\bar{q} \to \gamma\gamma$), gluon fusion ($gg \to \gamma\gamma$), and gluon-(anti)quark scattering ($qg \to \gamma\gamma q$) processes. One or both photons come either directly from the hard process or from parton fragmentation, in which a cascade of successive collinear splittings yields a radiated photon. Contributions from the quark-antiquark annihilation process and the single- and double-fragmentation processes are calculated up to order $\alpha_s\alpha^2$ with the DIPHOX 1.3.2 program [1]. The contributions from the gluon fusion process, including the one-loop box diagram of order $\alpha_s^2\alpha^2$, the interference between the one- and two-loop box diagrams, and the real emission one-loop "pentagon" $gg \to \gamma\gamma g$, both of order $\alpha_s^3\alpha^2$, are calculated with the GAMMA2MC 1.1.1 program [2]. The fragmentation function BFG set II [30] is used in the calculation. Although they are higher-order processes, the gluon fusion contributions are quantitatively comparable to those from quark-antiquark annihilation in the diphoton mass range of interest, due to the significant gluon luminosity in this mass range at the LHC. The three theoretical scales, renormalisation, initial factorisation, and fragmentation, are set to the diphoton mass value.

The photons are required to be within the kinematic acceptance defined in Section 1. An additional isolation requirement at the parton level is imposed by requiring the total hadronic transverse energy deposited in a cone of radius $R = 0.4$ centred on the photon direction to be less than 5 GeV. Particles resulting from underlying-event activity and hadronisation are not included in partonic event generators such as DIPHOX and GAMMA2MC. The fraction of diphotons not selected due to underlying hadronic activity falling inside the isolation cone is estimated using the PYTHIA 6.4.22 [12] event generator with tunes Z2, D6T [31], P0 [32], and DWT [31]. A factor of 0.95 ± 0.04 is applied to the parton-level cross section to correct for this effect.

The uncertainties associated with parton distribution functions and the strong coupling constant α_s are determined according to the PDF4LHC recommendations [33]. The diphoton cross section is computed with three different PDF sets (CT10 [34], MSTW08 [35], and NNPDF2.1 [36]), taking into account their associated uncertainties and the uncertainties on α_s. The respective preferred α_s central value of each PDF set is used, and α_s is varied by ± 0.012. The value for the cross section is taken as the midpoint of the envelope of the three results, including the uncertainties (68% confidence level envelope). The uncertainty on the cross section is taken to be the half-width of the envelope.

The theoretical scale uncertainties are estimated by varying the renormalisation, initial factorisation, and fragmentation scales by factors of 1/2 and 2, keeping the ratio between any two scales less than 2 (for example the combination $0.5\,m_{\gamma\gamma}$, $2\,m_{\gamma\gamma}$, $m_{\gamma\gamma}$ is not considered). The uncertainty is taken to be the maximum difference in the resulting cross sections.

8 Results

The integrated diphoton cross sections obtained for the acceptances defined in Section 1 are

$$\sigma(pp \to \gamma\gamma)|_{|\eta|<1.44} = 31.0 \pm 1.8\ \text{(stat.)}\ ^{+2.0}_{-2.1}\ \text{(syst.)} \pm 1.2\ \text{(lumi.)}\ \text{pb},$$

$$\sigma(pp \to \gamma\gamma)|_{|\eta|<2.50} = 62.4 \pm 3.6\ \text{(stat.)}\ ^{+5.3}_{-5.8}\ \text{(syst.)} \pm 2.5\ \text{(lumi.)}\ \text{pb}.$$

The theoretical calculation described in the previous section predicts

$$\sigma(pp \to \gamma\gamma)|_{|\eta|<1.44} = 27.3\ ^{+3.0}_{-2.2}\ \text{(scales)} \pm 1.1\ \text{(PDF)}\ \text{pb},$$

$$\sigma(pp \to \gamma\gamma)|_{|\eta|<2.50} = 52.7\ ^{+5.8}_{-4.2}\ \text{(scales)} \pm 2.0\ \text{(PDF)}\ \text{pb}.$$

The integrated cross sections obtained from the calculation are consistent with the measurements within the experimental and theoretical uncertainties.

The differential cross-section measurements as functions of $m_{\gamma\gamma}$, $\Delta\varphi_{\gamma\gamma}$, $p_{T,\gamma\gamma}$, and $|\cos\theta^*|$ for the two pseudorapidity ranges are shown, along with the theoretical predictions, in Figs. 3 to 10. The 4% uncertainty on the integrated luminosity is not included in the error bars. The values of the cross sections are given in Tables 2 to 5. As can be seen in Figs. 7 and 8, the theoretical predictions underestimate the measured cross section for $\Delta\varphi_{\gamma\gamma} < 2.8$. In the leading-order (LO) diagrams of gluon fusion and quark-antiquark annihilation $2 \to 2$ processes, the two photons are back-to-back because of momentum conservation. Therefore, the LO term does not contribute to this phase space region, which thus only receives contributions from NLO terms for both the direct and fragmentation diphoton production processes.

The contribution for $\Delta\varphi_{\gamma\gamma} \lesssim 2.8$, combined with the requirements of $E_T > 20$ and 23 GeV on the two photons, is responsible for the shoulder around 40 GeV in the diphoton differental p_T distribution of Figs. 5 and 6. This contribution also populates the region below 30 GeV in the diphoton mass distribution shown in Figs. 3 and 4. In these two regions of the $p_{T,\gamma\gamma}$ and $m_{\gamma\gamma}$ spectra, the theoretical cross section is lower than the measurement, consistent with the deficit for $\Delta\varphi_{\gamma\gamma} \lesssim 2.8$.

Comparison of the measurements of the $|\cos\theta^*|$ spectra with theoretical predictions, shown in Figs. 9 and 10, reveals an underestimation from the theory at large $|\cos\theta^*|$ values, which is more significant for the central rapidity range ($|\eta| < 1.44$). Similar discrepancies have previously been observed in diphoton production at hadron colliders [5, 8, 37] as discussed in Ref. [38].

Table 2: Measured diphoton differential cross section as a function of $m_{\gamma\gamma}$ for the two photon pseudorapidity ranges, with statistical (stat.) and systematic (syst.) uncertainties.

$d\sigma/dm_{\gamma\gamma}$ [pb/GeV]								
$m_{\gamma\gamma}$ [GeV]	$\|\eta\| < 1.44$				$\|\eta\| < 2.5$			
		stat.	syst.			stat.	syst.	
0−30	0.0299	±0.0071	+0.0069	−0.0086	0.050	±0.013	+0.014	−0.024
30−40	0.061	±0.030	+0.015	−0.018	0.127	±0.049	+0.035	−0.061
40−45	0.097	±0.088	+0.020	−0.020	0.28	±0.17	+0.06	−0.07
45−55	0.77	±0.12	+0.06	−0.05	1.40	±0.20	+0.14	−0.12
55−65	0.70	±0.10	+0.05	−0.04	1.43	±0.18	+0.10	−0.09
65−80	0.408	±0.059	+0.030	−0.031	0.80	±0.11	+0.07	−0.06
80−100	0.175	±0.031	+0.013	−0.012	0.365	±0.063	+0.041	−0.037
100−140	0.070	±0.012	+0.003	−0.003	0.142	±0.028	+0.020	−0.018
140−200	0.0102	±0.0035	+0.0007	−0.0006	0.054	±0.015	+0.006	−0.006
200−300	0.0022	±0.0011	+0.0001	−0.0001	0.0084	±0.0060	+0.0023	−0.0019

9 Summary

The integrated and differential production cross sections for isolated photon pairs have been measured in proton-proton collisions at a centre-of-mass energy of 7 TeV, using data collected

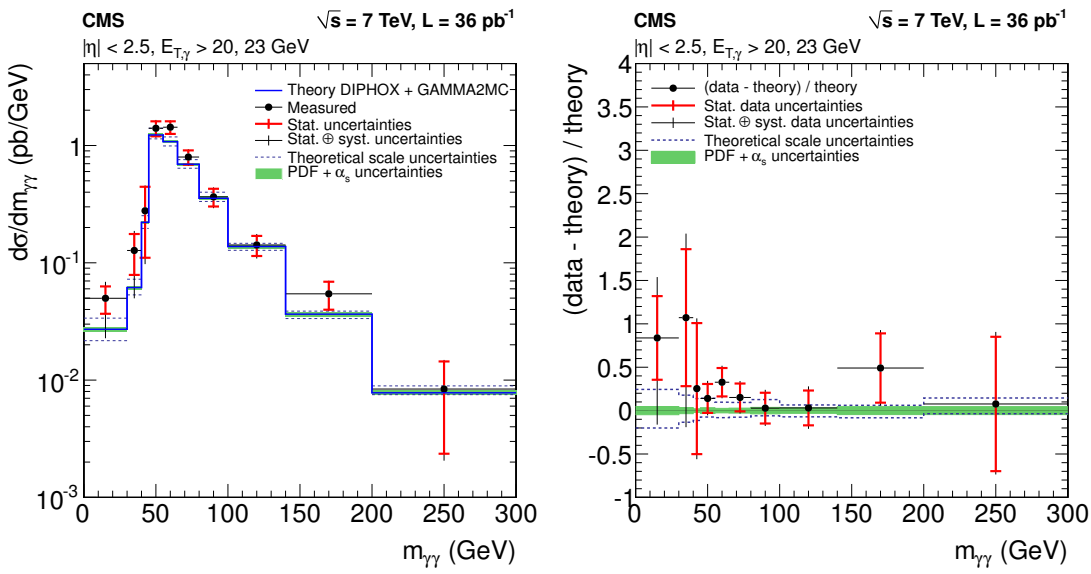

Figure 3: (Left) Diphoton differential cross section as a function of the photon pair invariant mass $m_{\gamma\gamma}$ from data (points) and from theory (solid line) for the photon pseudorapidity range $|\eta| < 2.5$. (Right) The difference between the measured and theoretically predicted diphoton cross sections, divided by the theory prediction, as a function of $m_{\gamma\gamma}$. In both plots, the inner and outer error bars on each point show the statistical and total experimental uncertainties. The 4% uncertainty on the integrated luminosity is not included in the error bars. The dotted line and shaded region represent the systematic uncertainties on the theoretical prediction from the theoretical scales and the PDFs, respectively.

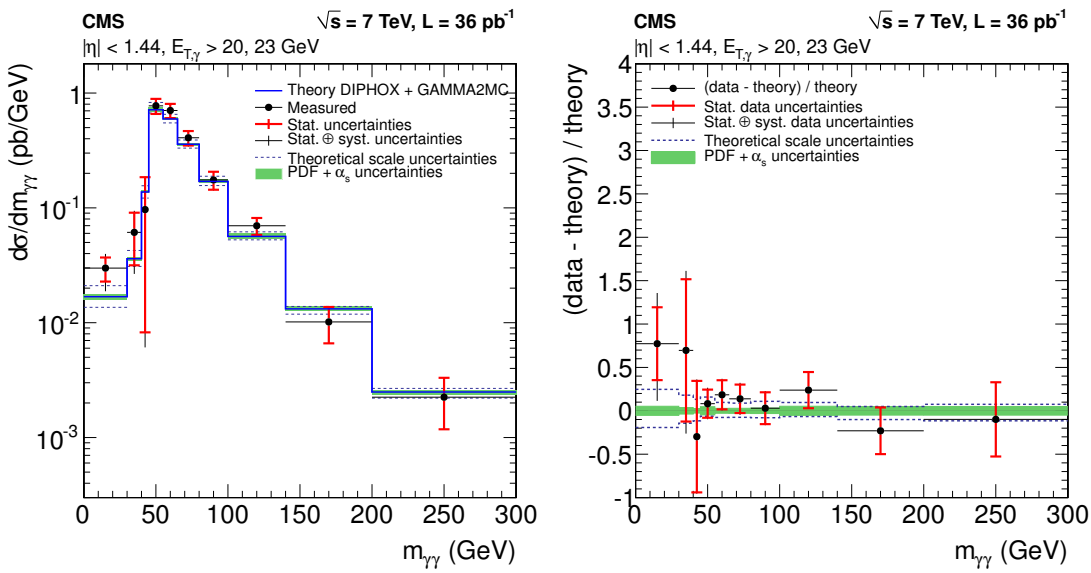

Figure 4: (Left) Diphoton differential cross section as a function of the photon pair invariant mass $m_{\gamma\gamma}$ from data (points) and from theory (solid line) for the photon pseudorapidity range $|\eta| < 1.44$. (Right) The difference between the measured and theoretically predicted diphoton cross sections, divided by the theory prediction, as a function of $m_{\gamma\gamma}$. In both plots, the inner and outer error bars on each point show the statistical and total experimental uncertainties. The 4% uncertainty on the integrated luminosity is not included in the error bars. The dotted line and shaded region represent the systematic uncertainties on the theoretical prediction from the theoretical scales and the PDFs, respectively.

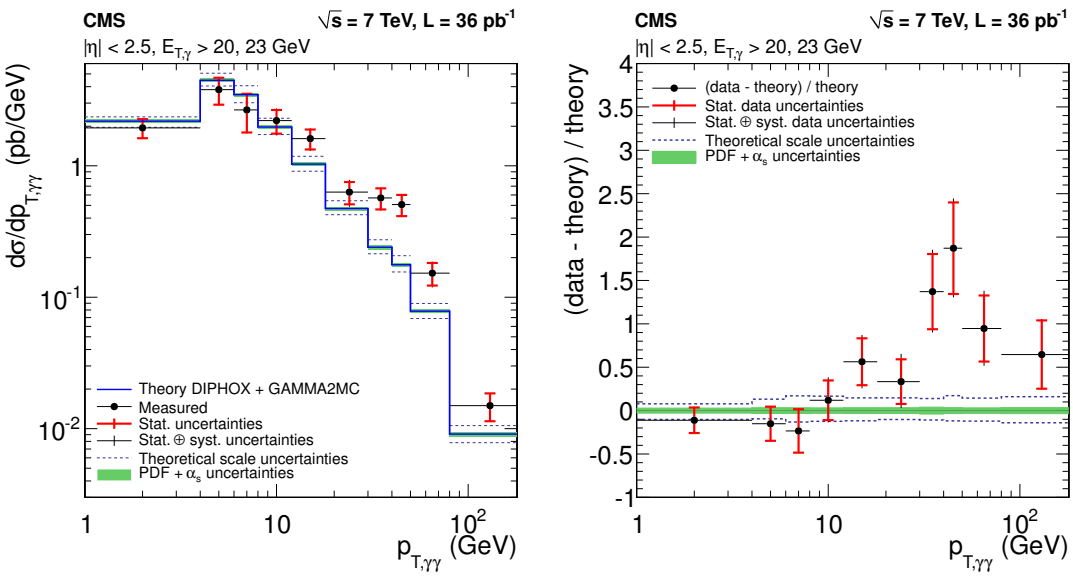

Figure 5: (Left) Diphoton differential cross section as a function of the photon pair transverse momentum $p_{T,\gamma\gamma}$ from data (points) and from theory (solid line) for the photon pseudorapidity range $|\eta| < 2.5$. (Right) The difference between the measured and theoretically predicted diphoton cross sections, divided by the theory prediction, as a function of $p_{T,\gamma\gamma}$. In both plots, the inner and outer error bars on each point show the statistical and total experimental uncertainties. The 4% uncertainty on the integrated luminosity is not included in the error bars. The dotted line and shaded region represent the systematic uncertainties on the theoretical prediction from the theoretical scales and the PDFs, respectively.

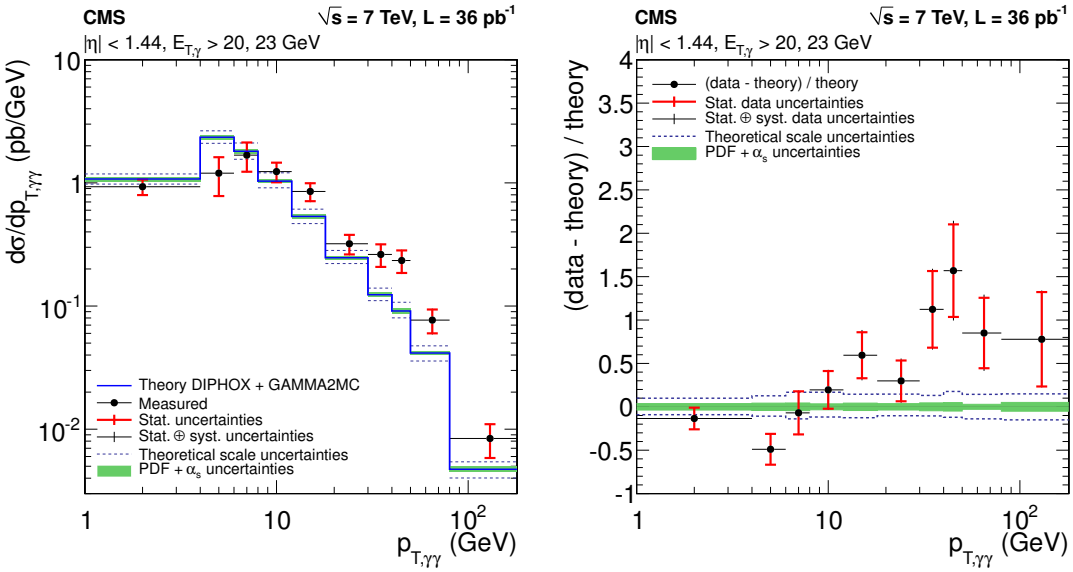

Figure 6: (Left) Diphoton differential cross section as a function of the photon pair transverse momentum $p_{T,\gamma\gamma}$ from data (points) and from theory (solid line) for the photon pseudorapidity range $|\eta| < 1.44$. (Right) The difference between the measured and theoretically predicted diphoton cross sections, divided by the theory prediction, as a function of $p_{T,\gamma\gamma}$. In both plots, the inner and outer error bars on each point show the statistical and total experimental uncertainties. The 4% uncertainty on the integrated luminosity is not included in the error bars. The dotted line and shaded region represent the systematic uncertainties on the theoretical prediction from the theoretical scales and the PDFs, respectively.

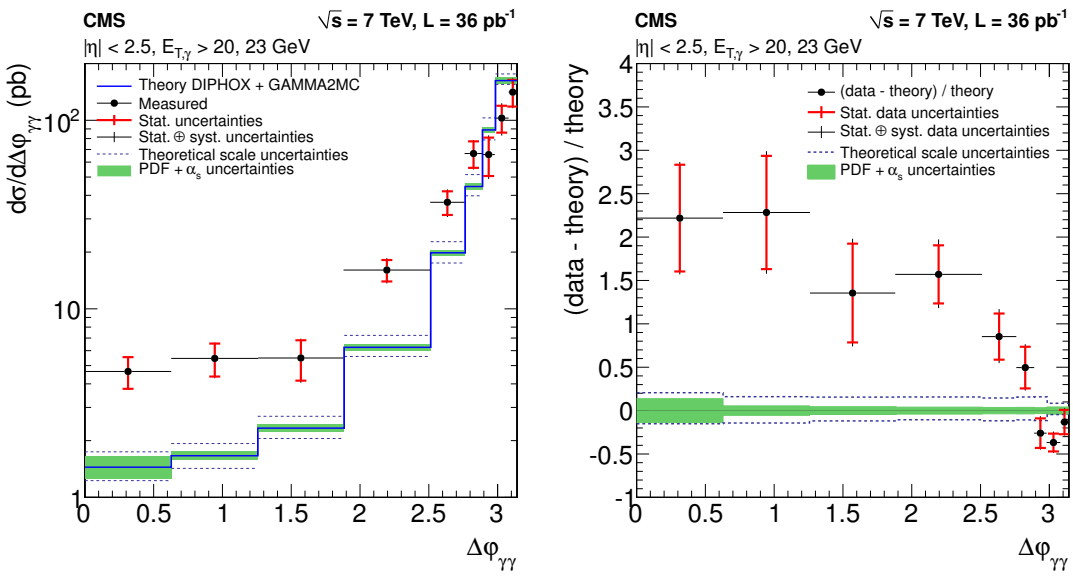

Figure 7: (Left) Diphoton differential cross section as a function of the azimuthal angle between the two photons, $\Delta\varphi_{\gamma\gamma}$, from data (points) and from theory (solid line) for the photon pseudorapidity range $|\eta| < 2.5$. (Right) The difference between the measured and theoretically predicted diphoton cross sections, divided by the theory prediction, as a function of $\Delta\varphi_{\gamma\gamma}$. In both plots, the inner and outer error bars on each point show the statistical and total experimental uncertainties. The 4% uncertainty on the integrated luminosity is not included in the error bars. The dotted line and shaded region represent the systematic uncertainties on the theoretical prediction from the theoretical scales and the PDFs, respectively.

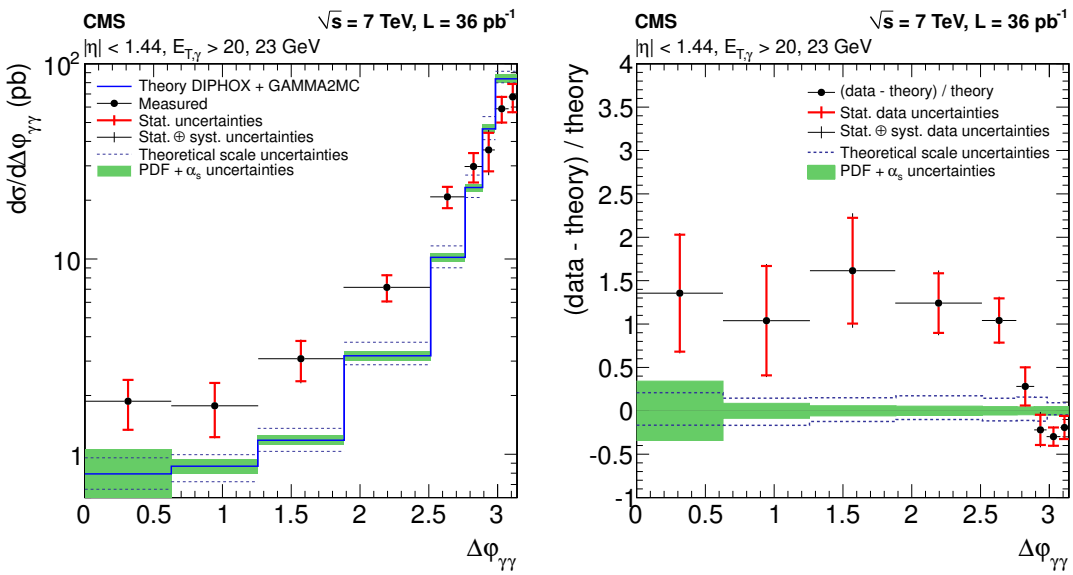

Figure 8: (Left) Diphoton differential cross section as a function of the azimuthal angle between the two photons, $\Delta\varphi_{\gamma\gamma}$, from data (points) and from theory (solid line) for the photon pseudorapidity range $|\eta| < 1.44$. (Right) The difference between the measured and theoretically predicted diphoton cross sections, divided by the theory prediction, as a function of $\Delta\varphi_{\gamma\gamma}$. In both plots, the inner and outer error bars on each point show the statistical and total experimental uncertainties. The 4% uncertainty on the integrated luminosity is not included in the error bars. The dotted line and shaded region represent the systematic uncertainties on the theoretical prediction from the theoretical scales and the PDFs, respectively.

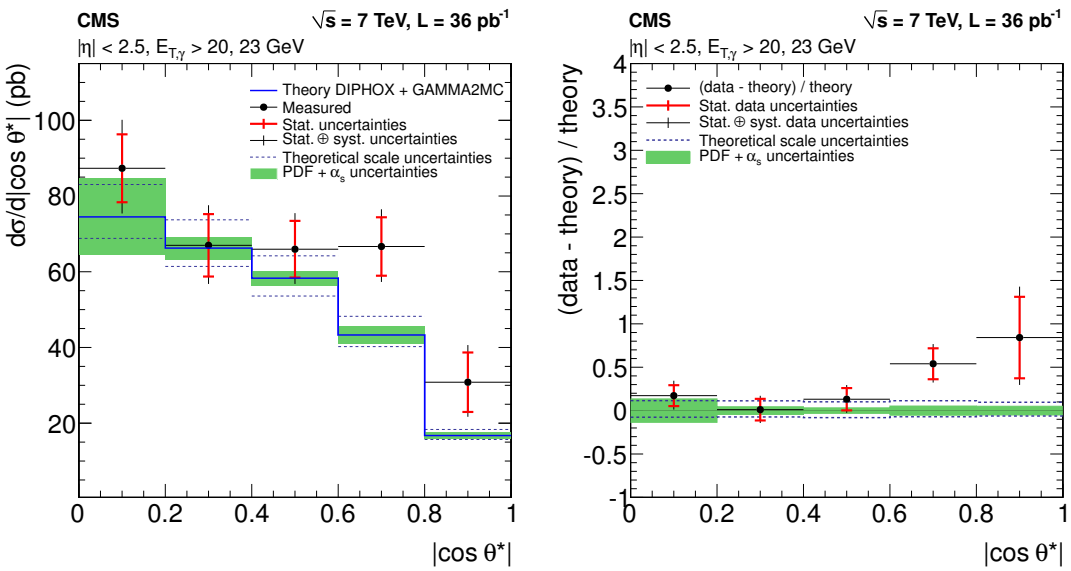

Figure 9: (Left) Diphoton differential cross section as a function of $|\cos\theta^*|$ from data (points) and from theory (solid line) for the photon pseudorapidity range $|\eta| < 2.5$. (Right) The difference between the measured and theoretically predicted diphoton cross sections, divided by the theory prediction, as a function of $|\cos\theta^*|$. In both plots, the inner and outer error bars on each point show the statistical and total experimental uncertainties. The 4% uncertainty on the integrated luminosity is not included in the error bars. The dotted line and shaded region represent the systematic uncertainties on the theoretical prediction from the theoretical scales and the PDFs, respectively.

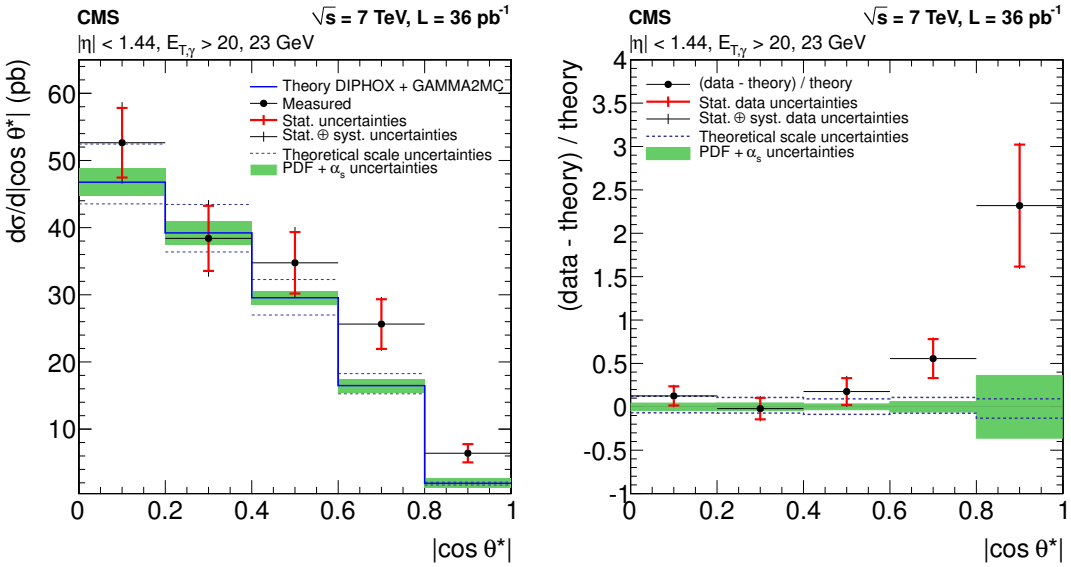

Figure 10: (Left) Diphoton differential cross section as a function of $|\cos\theta^*|$ from data (points) and from theory (solid line) for the photon pseudorapidity range $|\eta| < 1.44$. (Right) The difference between the measured and theoretically predicted diphoton cross sections, divided by the theory prediction, as a function of $|\cos\theta^*|$. In both plots, the inner and outer error bars on each point show the statistical and total experimental uncertainties. The 4% uncertainty on the integrated luminosity is not included in the error bars. The dotted line and shaded region represent the systematic uncertainties on the theoretical prediction from the theoretical scales and the PDFs, respectively.

Table 3: Measured diphoton differential cross section as a function of $p_{T,\gamma\gamma}$ for the two photon pseudorapidity ranges, with statistical (stat.) and systematic (syst.) uncertainties.

$d\sigma/dp_{T,\gamma\gamma}$ [pb/GeV]								
$p_{T,\gamma\gamma}$ [GeV]	$\lvert\eta\rvert < 1.44$				$\lvert\eta\rvert < 2.5$			
		stat.	syst.			stat.	syst.	
0−4	0.93	±0.13	+0.04	−0.05	1.94	±0.32	+0.12	−0.13
4−6	1.20	±0.42	+0.10	−0.09	3.80	±0.88	+0.27	−0.29
6−8	1.68	±0.45	+0.12	−0.12	2.66	±0.87	+0.27	−0.24
8−12	1.24	±0.22	+0.08	−0.08	2.21	±0.45	+0.26	−0.22
12−18	0.85	±0.14	+0.06	−0.06	1.61	±0.28	+0.15	−0.15
18−30	0.320	±0.058	+0.026	−0.022	0.63	±0.12	+0.09	−0.08
30−40	0.262	±0.055	+0.019	−0.017	0.57	±0.10	+0.05	−0.04
40−50	0.234	±0.049	+0.020	−0.019	0.507	±0.093	+0.040	−0.036
50−80	0.077	±0.017	+0.007	−0.007	0.153	±0.030	+0.016	−0.016
80−180	0.0084	±0.0026	+0.0006	−0.0005	0.0150	±0.0036	+0.0010	−0.0009

Table 4: Measured diphoton differential cross section as a function of $\Delta\phi_{\gamma\gamma}$ for the two photon pseudorapidity ranges, with statistical (stat.) and systematic (syst.) uncertainties.

$d\sigma/d\Delta\phi_{\gamma\gamma}$ [pb]								
$\Delta\phi_{\gamma\gamma}$	$\lvert\eta\rvert < 1.44$				$\lvert\eta\rvert < 2.5$			
		stat.	syst.			stat.	syst.	
$0-0.2\pi$	1.87	±0.53	+0.13	−0.13	4.65	±0.89	+0.29	−0.30
$0.2\pi-0.4\pi$	1.77	±0.55	+0.15	−0.14	5.5	±1.1	+0.5	−0.4
$0.4\pi-0.6\pi$	3.09	±0.72	+0.31	−0.29	5.5	±1.3	+0.6	−0.5
$0.6\pi-0.8\pi$	7.2	±1.1	+0.5	−0.4	16.1	±2.1	+1.4	−1.2
$0.8\pi-0.88\pi$	20.8	±2.6	+1.0	−1.0	36.7	±5.3	+3.4	−3.0
$0.88\pi-0.92\pi$	29.8	±5.1	+1.7	−1.5	67	±11	+5	−5
$0.92\pi-0.95\pi$	36.2	±8.1	+5.1	−4.7	66	±15	+9	−8
$0.95\pi-0.98\pi$	58.8	±8.8	+4.2	−3.8	103	±17	+12	−11
$0.98\pi-\pi$	68	±11	+4	−4	141	±23	+12	−11

Table 5: Measured diphoton differential cross section as a function of $|\cos\theta^*|$ for the two photon pseudorapidity ranges, with statistical (stat.) and systematic (syst.) uncertainties.

$d\sigma/d\|\cos\theta^*\|$ [pb]								
$\|\cos\theta^*\|$	$\|\eta\| < 1.44$				$\|\eta\| < 2.5$			
		stat.	syst.			stat.	syst.	
0−0.2	52.6	±5.2	+3.1	−3.2	87.3	±9.0	+9.1	−7.9
0.2−0.4	38.4	±4.9	+3.0	−3.0	67.0	±8.2	+6.6	−6.0
0.4−0.6	34.8	±4.6	+2.7	−2.5	66.0	±7.5	+5.9	−5.3
0.6−0.8	25.6	±3.7	+1.6	−1.5	66.7	±7.7	+6.1	−5.3
0.8−1	6.4	±1.4	+0.3	−0.4	30.8	±7.9	+5.9	−4.7

by the CMS detector in 2010, corresponding to an integrated luminosity of $36\,\mathrm{pb}^{-1}$. The differential cross sections have been measured as functions of the diphoton invariant mass, the diphoton transverse momentum, the difference between the two photon azimuthal angles, and $|\cos\theta^*|$. The background from hadron decay products was estimated with a statistical method based on an electromagnetic energy isolation variable $\mathcal{I}$. The signal and background distributions for $\mathcal{I}$ were entirely extracted from data, resulting in systematic uncertainties of approximately 10% on the measured diphoton yields.

The measurements have been compared to a theoretical prediction performed at next-to-leading-order accuracy using the state-of-the-art fixed-order computations [1, 2]. Whereas there is an overall agreement between theory and data for the diphoton mass spectrum, the theory underestimates the cross section in regions of the phase space where the two photons have an azimuthal angle difference $\Delta\varphi \lesssim 2.8$.

Acknowledgements

We wish to express our gratitude to J-Ph. Guillet, E. Pilon, Z. Bern, L. Dixon, and C. Schmidt for the fruitful discussions on the theoretical aspects concerning the measurement.

We wish to congratulate our colleagues in the CERN accelerator departments for the excellent performance of the LHC machine. We thank the technical and administrative staff at CERN and other CMS institutes, and acknowledge support from: FMSR (Austria); FNRS and FWO (Belgium); CNPq, CAPES, FAPERJ, and FAPESP (Brazil); MES (Bulgaria); CERN; CAS, MoST, and NSFC (China); COLCIENCIAS (Colombia); MSES (Croatia); RPF (Cyprus); Academy of Sciences and NICPB (Estonia); Academy of Finland, MEC, and HIP (Finland); CEA and CNRS/IN2P3 (France); BMBF, DFG, and HGF (Germany); GSRT (Greece); OTKA and NKTH (Hungary); DAE and DST (India); IPM (Iran); SFI (Ireland); INFN (Italy); NRF and WCU (Korea); LAS (Lithuania); CINVESTAV, CONACYT, SEP, and UASLP-FAI (Mexico); MSI (New Zealand); PAEC (Pakistan); SCSR (Poland); FCT (Portugal); JINR (Armenia, Belarus, Georgia, Ukraine, Uzbekistan); MST, MAE and RFBR (Russia); MSTD (Serbia); MICINN and CPAN (Spain); Swiss Funding Agencies (Switzerland); NSC (Taipei); TUBITAK and TAEK (Turkey); STFC (United Kingdom); DOE and NSF (USA). Individuals have received support from the Marie-Curie programme and the European Research Council (European Union); the Leventis Foundation; the A. P. Sloan Foundation; the Alexander von Humboldt Foundation; the Belgian Federal Science Policy Office; the Fonds pour la Formation à la Recherche dans l'Industrie et dans l'Agriculture (FRIA-

Belgium); the Agentschap voor Innovatie door Wetenschap en Technologie (IWT-Belgium); and the Council of Science and Industrial Research, India.

References

[1] T. Binoth, J. P. Guillet, E. Pilon et al., "A full next-to-leading order study of direct photon pair production in hadronic collisions", *Eur. Phys. J. C* **16** (2000) 311, arXiv:hep-ph/9911340. doi:10.1007/s100520050024.

[2] Z. Bern, L. J. Dixon, and C. Schmidt, "Isolating a light Higgs boson from the di-photon background at the CERN LHC", *Phys. Rev. D* **66** (2002) 074018, arXiv:hep-ph/0206194. doi:10.1103/PhysRevD.66.074018.

[3] V. Saleev, "Diphoton production at Tevatron in the quasi-multi-Regge-kinematics approach", *Phys. Rev. D* **80** (2009) 114016, arXiv:0911.5517. doi:10.1103/PhysRevD.80.114016.

[4] C. Balázs, E. Berger, P. Nadolsky et al., "Calculation of prompt diphoton production cross sections at Tevatron and CERN LHC energies", *Phys. Rev. D* **76** (2007) 013009, arXiv:0704.0001. doi:10.1103/PhysRevD.76.013009.

[5] D0 Collaboration, "Measurement of direct photon pair production cross sections in $p\bar{p}$ collisions at $\sqrt{s} = 1.96$ TeV", *Phys. Lett. B* **690** (2010) 108, arXiv:1002.4917. doi:10.1016/j.physletb.2010.05.017.

[6] CDF Collaboration, "Measurement of the Cross Section for Prompt Isolated Diphoton Production in $p\overline{p}$ Collisions at $\sqrt{s} = 1.96$ TeV", *Phys. Rev. Lett.* **107** (2011) 102003. doi:10.1103/PhysRevLett.107.102003.

[7] CDF Collaboration, "Measurement of the cross section for prompt isolated diphoton production in $p\overline{p}$ collisions at $\sqrt{s} = 1.96$ TeV", *Phys. Rev. D* **84** (2011) 052006. doi:10.1103/PhysRevD.84.052006.

[8] ATLAS Collaboration, "Measurement of the isolated di-photon cross-section in pp collisions at sqrt(s) = 7 TeV with the ATLAS detector", (2011). arXiv:1107.0581. Submitted to *Phys. Rev. D*.

[9] CMS Collaboration, "The CMS experiment at the CERN LHC", *JINST* **03** (2008) S08004. doi:10.1088/1748-0221/3/08/S08004.

[10] S. Frixione and G. Ridolfi, "Jet photoproduction at HERA", *Nucl. Phys. B* **507** (1997) 315, arXiv:hep-ph/9707345. doi:10.1016/S0550-3213(97)00575-0.

[11] M. Fontannaz, J. Guillet, and G. Heinrich, "Is a large intrinsic k(T) needed to describe photon + jet photoproduction at HERA?", *Eur. Phys. J. C* **22** (2001) 303, arXiv:hep-ph/0107262. doi:10.1007/s100520100797.

[12] T. Sjöstrand, S. Mrenna, and P. Skands, "PYTHIA 6.4 Physics and Manual", *JHEP* **05** (2006) 026, arXiv:hep-ph/0603175. doi:10.1088/1126-6708/2006/05/026.

[13] J. Pumplin, D. Stump, J. Huston et al., "New generation of parton distributions with uncertainties from global QCD analysis", *JHEP* **07** (2002) 012, arXiv:hep-ph/0201195. doi:10.1088/1126-6708/2002/07/012.

[14] Geant4 Collaboration, "The GEANT4 Toolkit: Simulation capabilities and application results", *Nucl. Phys. Proc. Suppl.* **125** (2003) 60. doi:10.1016/S0920-5632(03)90967-4.

[15] R. Field, "Early LHC Underlying Event Data – Findings and Surprises", (2010). arXiv:1010.3558.

[16] H. Lai, J. Huston, S. Kuhlmann et al., "Global QCD analysis of parton structure of the nucleon: CTEQ5 parton distributions", *Eur. Phys. J. C* **12** (2000) 375. doi:10.1007/s100529900196.

[17] CMS Collaboration, "Photon reconstruction and identification at $\sqrt{s}$ = 7 TeV", CMS Physics Analysis Summary CMS-PAS-EGM-10-005, (2010).

[18] CMS Collaboration, "Isolated Photon Reconstruction and Identification at $\sqrt{s} = 7$ TeV", CMS Physics Analysis Summary CMS-PAS-EGM-10-006, (2010).

[19] S. Alioli, P. Nason, C. Oleari et al., "A general framework for implementing NLO calculations in shower Monte Carlo programs: the POWHEG BOX", *JHEP* **06** (2010) 043, arXiv:1002.2581. doi:10.1007/JHEP06(2010)043.

[20] S. Frixione, P. Nason, and C. Oleari, "Matching NLO QCD computations with Parton Shower simulations: the POWHEG method", *JHEP* **11** (2007) 070, arXiv:0709.2092. doi:10.1088/1126-6708/2007/11/070.

[21] P. Nason, "A new method for combining NLO QCD with shower Monte Carlo algorithms", *JHEP* **11** (2004) 040, arXiv:hep-ph/0409146. doi:10.1088/1126-6708/2004/11/040.

[22] CMS Collaboration, "Measurement of the Drell–Yan cross section in pp collisions at $\sqrt{s} = 7$ TeV", *JHEP* **11** (2011) 1. doi:10.1007/JHEP10(2011)007.

[23] M. Pivk and F. R. Le Diberder, "sPlot: a statistical tool to unfold data distributions", *Nucl. Instrum. Meth. A* **555** (2005) 356, arXiv:physics/0402083. doi:10.1016/j.nima.2005.08.106.

[24] W. Eadie, D. Drijard, F. James et al., "Statistical methods in experimental physics". North-Holland publishing company, 1977.

[25] G. Cowan, "Statistical Data Analysis", ch. 1. Clarendon Press, Oxford, 1998.

[26] CMS Collaboration, "Measurements of Inclusive W and Z Cross Sections in pp Collisions at $\sqrt{s} = 7$ TeV", *JHEP* **01** (2011) 080, arXiv:1012.2466. doi:10.1007/JHEP01(2011)080.

[27] CMS Collaboration, "Electron Reconstruction and Identification at $\sqrt{s} = 7$ TeV", CMS Physics Analysis Summary CMS-PAS-EGM-10-004, (2010).

[28] CMS Collaboration, "ECAL 2010 performance results", CMS Detector Performance Summary CERN-CMS-DP-2011-008, (2011).

[29] CMS Collaboration, "Absolute luminosity normalization", CMS Detector Performance Summary CERN-CMS-DP-2011-002, (2011).

[30] L. Bourhis, M. Fontannaz, and J. P. Guillet, "Quark and gluon fragmentation functions into photons", *Eur. Phys. J.* **C2** (1998) 529, arXiv:hep-ph/9704447. doi:10.1007/s100520050158.

[31] CDF Collaboration, R. Field, "Studying the *underlying event* at CDF and the LHC", in *Multiple partonic interactions at the LHC. Proceedings, 1st International Workshop, MPI'08, Perugia, Italy, October 27-31, 2008*, P. Bartalini and L. Fanó, eds., p. 9. 2010. arXiv:1003.4220. DESY-PROC-2009-06.

[32] P. Z. Skands, "Tuning Monte Carlo Generators: The Perugia Tunes", *Phys. Rev. D* **82** (2010) 074018, arXiv:1005.3457. doi:10.1103/PhysRevD.82.074018.

[33] PDF4LHC Working Group Collaboration, "The PDF4LHC Working Group Interim Recommendations", (2011). arXiv:1101.0538.

[34] H.-L. Lai, M. Guzzi, J. Huston et al., "New parton distributions for collider physics", *Phys. Rev. D* **82** (2010) 074024, arXiv:1007.2241. doi:10.1103/PhysRevD.82.074024.

[35] A. D. Martin, W. J. Stirling, R. S. Thorne et al., "Parton distributions for the LHC", *Eur. Phys. J. C* **63** (2009) 189, arXiv:0901.0002. doi:10.1140/epjc/s10052-009-1072-5.

[36] NNPDF Collaboration, "Impact of Heavy Quark Masses on Parton Distributions and LHC Phenomenology", *Nucl. Phys. B* **849** (2011) 296, arXiv:1101.1300. doi:10.1016/j.nuclphysb.2011.03.021.

[37] CDF Collaboration, "Measurement of the Cross Section for Prompt Isolated Diphoton Production in $p\bar{p}$ Collisions at $\sqrt{s} = 1.96$ TeV", *Phys. Rev. Lett.* **107** (2011) 102003, arXiv:1106.5123. doi:10.1103/PhysRevLett.107.102003.

[38] T. Binoth et al., "Beyond leading order effects in photon pair production at the Tevatron", *Phys. Rev. D* **63** (2001) 114016, arXiv:hep-ph/0012191. doi:10.1103/PhysRevD.63.114016.

A The CMS Collaboration

Yerevan Physics Institute, Yerevan, Armenia
S. Chatrchyan, V. Khachatryan, A.M. Sirunyan, A. Tumasyan

Institut für Hochenergiephysik der OeAW, Wien, Austria
W. Adam, T. Bergauer, M. Dragicevic, J. Erö, C. Fabjan, M. Friedl, R. Frühwirth, V.M. Ghete, J. Hammer[1], M. Hoch, N. Hörmann, J. Hrubec, M. Jeitler, W. Kiesenhofer, A. Knapitsch, M. Krammer, D. Liko, I. Mikulec, M. Pernicka[†], B. Rahbaran, H. Rohringer, R. Schöfbeck, J. Strauss, A. Taurok, F. Teischinger, C. Trauner, P. Wagner, W. Waltenberger, G. Walzel, E. Widl, C.-E. Wulz

National Centre for Particle and High Energy Physics, Minsk, Belarus
V. Mossolov, N. Shumeiko, J. Suarez Gonzalez

Universiteit Antwerpen, Antwerpen, Belgium
S. Bansal, L. Benucci, T. Cornelis, E.A. De Wolf, X. Janssen, S. Luyckx, T. Maes, L. Mucibello, S. Ochesanu, B. Roland, R. Rougny, M. Selvaggi, H. Van Haevermaet, P. Van Mechelen, N. Van Remortel, A. Van Spilbeeck

Vrije Universiteit Brussel, Brussel, Belgium
F. Blekman, S. Blyweert, J. D'Hondt, R. Gonzalez Suarez, A. Kalogeropoulos, M. Maes, A. Olbrechts, W. Van Doninck, P. Van Mulders, G.P. Van Onsem, I. Villella

Université Libre de Bruxelles, Bruxelles, Belgium
O. Charaf, B. Clerbaux, G. De Lentdecker, V. Dero, A.P.R. Gay, G.H. Hammad, T. Hreus, A. Léonard, P.E. Marage, L. Thomas, C. Vander Velde, P. Vanlaer, J. Wickens

Ghent University, Ghent, Belgium
V. Adler, K. Beernaert, A. Cimmino, S. Costantini, M. Grunewald, B. Klein, J. Lellouch, A. Marinov, J. Mccartin, A.A. Ocampo Rios, D. Ryckbosch, N. Strobbe, F. Thyssen, M. Tytgat, L. Vanelderen, P. Verwilligen, S. Walsh, N. Zaganidis

Université Catholique de Louvain, Louvain-la-Neuve, Belgium
S. Basegmez, G. Bruno, J. Caudron, L. Ceard, J. De Favereau De Jeneret, C. Delaere, D. Favart, L. Forthomme, A. Giammanco[2], G. Grégoire, J. Hollar, V. Lemaitre, J. Liao, O. Militaru, C. Nuttens, D. Pagano, A. Pin, K. Piotrzkowski, N. Schul

Université de Mons, Mons, Belgium
N. Beliy, T. Caebergs, E. Daubie

Centro Brasileiro de Pesquisas Fisicas, Rio de Janeiro, Brazil
G.A. Alves, D. De Jesus Damiao, M.E. Pol, M.H.G. Souza

Universidade do Estado do Rio de Janeiro, Rio de Janeiro, Brazil
W.L. Aldá Júnior, W. Carvalho, A. Custódio, E.M. Da Costa, C. De Oliveira Martins, S. Fonseca De Souza, D. Matos Figueiredo, L. Mundim, H. Nogima, V. Oguri, W.L. Prado Da Silva, A. Santoro, S.M. Silva Do Amaral, A. Sznajder

Instituto de Fisica Teorica, Universidade Estadual Paulista, Sao Paulo, Brazil
T.S. Anjos[3], C.A. Bernardes[3], F.A. Dias[4], T.R. Fernandez Perez Tomei, E. M. Gregores[3], C. Lagana, F. Marinho, P.G. Mercadante[3], S.F. Novaes, Sandra S. Padula

Institute for Nuclear Research and Nuclear Energy, Sofia, Bulgaria
N. Darmenov[1], V. Genchev[1], P. Iaydjiev[1], S. Piperov, M. Rodozov, S. Stoykova, G. Sultanov, V. Tcholakov, R. Trayanov, M. Vutova

University of Sofia, Sofia, Bulgaria
A. Dimitrov, R. Hadjiiska, A. Karadzhinova, V. Kozhuharov, L. Litov, B. Pavlov, P. Petkov

Institute of High Energy Physics, Beijing, China
J.G. Bian, G.M. Chen, H.S. Chen, C.H. Jiang, D. Liang, S. Liang, X. Meng, J. Tao, J. Wang, J. Wang, X. Wang, Z. Wang, H. Xiao, M. Xu, J. Zang, Z. Zhang

State Key Lab. of Nucl. Phys. and Tech., Peking University, Beijing, China
Y. Ban, S. Guo, Y. Guo, W. Li, S. Liu, Y. Mao, S.J. Qian, H. Teng, S. Wang, B. Zhu, W. Zou

Universidad de Los Andes, Bogota, Colombia
A. Cabrera, B. Gomez Moreno, A.F. Osorio Oliveros, J.C. Sanabria

Technical University of Split, Split, Croatia
N. Godinovic, D. Lelas, R. Plestina[5], D. Polic, I. Puljak[1]

University of Split, Split, Croatia
Z. Antunovic, M. Dzelalija, M. Kovac

Institute Rudjer Boskovic, Zagreb, Croatia
V. Brigljevic, S. Duric, K. Kadija, J. Luetic, S. Morovic

University of Cyprus, Nicosia, Cyprus
A. Attikis, M. Galanti, J. Mousa, C. Nicolaou, F. Ptochos, P.A. Razis

Charles University, Prague, Czech Republic
M. Finger, M. Finger Jr.

Academy of Scientific Research and Technology of the Arab Republic of Egypt, Egyptian Network of High Energy Physics, Cairo, Egypt
Y. Assran[6], A. Ellithi Kamel[7], S. Khalil[8], M.A. Mahmoud[9], A. Radi[10]

National Institute of Chemical Physics and Biophysics, Tallinn, Estonia
A. Hektor, M. Kadastik, M. Müntel, M. Raidal, L. Rebane, A. Tiko

Department of Physics, University of Helsinki, Helsinki, Finland
V. Azzolini, P. Eerola, G. Fedi, M. Voutilainen

Helsinki Institute of Physics, Helsinki, Finland
S. Czellar, J. Härkönen, A. Heikkinen, V. Karimäki, R. Kinnunen, M.J. Kortelainen, T. Lampén, K. Lassila-Perini, S. Lehti, T. Lindén, P. Luukka, T. Mäenpää, E. Tuominen, J. Tuominiemi, E. Tuovinen, D. Ungaro, L. Wendland

Lappeenranta University of Technology, Lappeenranta, Finland
K. Banzuzi, A. Korpela, T. Tuuva

Laboratoire d'Annecy-le-Vieux de Physique des Particules, IN2P3-CNRS, Annecy-le-Vieux, France
D. Sillou

DSM/IRFU, CEA/Saclay, Gif-sur-Yvette, France
M. Besancon, S. Choudhury, M. Dejardin, D. Denegri, B. Fabbro, J.L. Faure, F. Ferri, S. Ganjour, A. Givernaud, P. Gras, G. Hamel de Monchenault, P. Jarry, E. Locci, J. Malcles, M. Marionneau, L. Millischer, J. Rander, A. Rosowsky, I. Shreyber, M. Titov

Laboratoire Leprince-Ringuet, Ecole Polytechnique, IN2P3-CNRS, Palaiseau, France
S. Baffioni, F. Beaudette, L. Benhabib, L. Bianchini, M. Bluj[11], C. Broutin, P. Busson, C. Charlot,

N. Daci, T. Dahms, L. Dobrzynski, S. Elgammal, R. Granier de Cassagnac, M. Haguenauer, P. Miné, C. Mironov, C. Ochando, P. Paganini, D. Sabes, R. Salerno, Y. Sirois, C. Thiebaux, C. Veelken, A. Zabi

Institut Pluridisciplinaire Hubert Curien, Université de Strasbourg, Université de Haute Alsace Mulhouse, CNRS/IN2P3, Strasbourg, France
J.-L. Agram[12], J. Andrea, D. Bloch, D. Bodin, J.-M. Brom, M. Cardaci, E.C. Chabert, C. Collard, E. Conte[12], F. Drouhin[12], C. Ferro, J.-C. Fontaine[12], D. Gelé, U. Goerlach, S. Greder, P. Juillot, M. Karim[12], A.-C. Le Bihan, P. Van Hove

Centre de Calcul de l'Institut National de Physique Nucleaire et de Physique des Particules (IN2P3), Villeurbanne, France
F. Fassi, D. Mercier

Université de Lyon, Université Claude Bernard Lyon 1, CNRS-IN2P3, Institut de Physique Nucléaire de Lyon, Villeurbanne, France
C. Baty, S. Beauceron, N. Beaupere, M. Bedjidian, O. Bondu, G. Boudoul, D. Boumediene, H. Brun, J. Chasserat, R. Chierici[1], D. Contardo, P. Depasse, H. El Mamouni, A. Falkiewicz, J. Fay, S. Gascon, M. Gouzevitch, B. Ille, T. Kurca, T. Le Grand, M. Lethuillier, L. Mirabito, S. Perries, V. Sordini, S. Tosi, Y. Tschudi, P. Verdier, S. Viret

Institute of High Energy Physics and Informatization, Tbilisi State University, Tbilisi, Georgia
D. Lomidze

RWTH Aachen University, I. Physikalisches Institut, Aachen, Germany
G. Anagnostou, S. Beranek, M. Edelhoff, L. Feld, N. Heracleous, O. Hindrichs, R. Jussen, K. Klein, J. Merz, A. Ostapchuk, A. Perieanu, F. Raupach, J. Sammet, S. Schael, D. Sprenger, H. Weber, B. Wittmer, V. Zhukov[13]

RWTH Aachen University, III. Physikalisches Institut A, Aachen, Germany
M. Ata, E. Dietz-Laursonn, M. Erdmann, T. Hebbeker, C. Heidemann, K. Hoepfner, T. Klimkovich, D. Klingebiel, P. Kreuzer, D. Lanske[†], J. Lingemann, C. Magass, M. Merschmeyer, A. Meyer, P. Papacz, H. Pieta, H. Reithler, S.A. Schmitz, L. Sonnenschein, J. Steggemann, D. Teyssier, M. Weber

RWTH Aachen University, III. Physikalisches Institut B, Aachen, Germany
M. Bontenackels, V. Cherepanov, M. Davids, G. Flügge, H. Geenen, M. Geisler, W. Haj Ahmad, F. Hoehle, B. Kargoll, T. Kress, Y. Kuessel, A. Linn, A. Nowack, L. Perchalla, O. Pooth, J. Rennefeld, P. Sauerland, A. Stahl, D. Tornier, M.H. Zoeller

Deutsches Elektronen-Synchrotron, Hamburg, Germany
M. Aldaya Martin, W. Behrenhoff, U. Behrens, M. Bergholz[14], A. Bethani, K. Borras, A. Cakir, A. Campbell, E. Castro, D. Dammann, G. Eckerlin, D. Eckstein, A. Flossdorf, G. Flucke, A. Geiser, J. Hauk, H. Jung[1], M. Kasemann, P. Katsas, C. Kleinwort, H. Kluge, A. Knutsson, M. Krämer, D. Krücker, E. Kuznetsova, W. Lange, W. Lohmann[14], B. Lutz, R. Mankel, I. Marfin, M. Marienfeld, I.-A. Melzer-Pellmann, A.B. Meyer, J. Mnich, A. Mussgiller, S. Naumann-Emme, J. Olzem, A. Petrukhin, D. Pitzl, A. Raspereza, P.M. Ribeiro Cipriano, M. Rosin, J. Salfeld-Nebgen, R. Schmidt[14], T. Schoerner-Sadenius, N. Sen, A. Spiridonov, M. Stein, J. Tomaszewska, R. Walsh, C. Wissing

University of Hamburg, Hamburg, Germany
C. Autermann, V. Blobel, S. Bobrovskyi, J. Draeger, H. Enderle, U. Gebbert, M. Görner, T. Hermanns, K. Kaschube, G. Kaussen, H. Kirschenmann, R. Klanner, J. Lange, B. Mura,

F. Nowak, N. Pietsch, C. Sander, H. Schettler, P. Schleper, E. Schlieckau, M. Schröder, T. Schum, H. Stadie, G. Steinbrück, J. Thomsen

Institut für Experimentelle Kernphysik, Karlsruhe, Germany
C. Barth, J. Berger, T. Chwalek, W. De Boer, A. Dierlamm, G. Dirkes, M. Feindt, J. Gruschke, M. Guthoff[1], C. Hackstein, F. Hartmann, M. Heinrich, H. Held, K.H. Hoffmann, S. Honc, I. Katkov[13], J.R. Komaragiri, T. Kuhr, D. Martschei, S. Mueller, Th. Müller, M. Niegel, O. Oberst, A. Oehler, J. Ott, T. Peiffer, G. Quast, K. Rabbertz, F. Ratnikov, N. Ratnikova, M. Renz, S. Röcker, C. Saout, A. Scheurer, P. Schieferdecker, F.-P. Schilling, M. Schmanau, G. Schott, H.J. Simonis, F.M. Stober, D. Troendle, J. Wagner-Kuhr, T. Weiler, M. Zeise, E.B. Ziebarth

Institute of Nuclear Physics "Demokritos", Aghia Paraskevi, Greece
G. Daskalakis, T. Geralis, S. Kesisoglou, A. Kyriakis, D. Loukas, I. Manolakos, A. Markou, C. Markou, C. Mavrommatis, E. Ntomari, E. Petrakou

University of Athens, Athens, Greece
L. Gouskos, T.J. Mertzimekis, A. Panagiotou, N. Saoulidou, E. Stiliaris

University of Ioánnina, Ioánnina, Greece
I. Evangelou, C. Foudas[1], P. Kokkas, N. Manthos, I. Papadopoulos, V. Patras, F.A. Triantis

KFKI Research Institute for Particle and Nuclear Physics, Budapest, Hungary
A. Aranyi, G. Bencze, L. Boldizsar, C. Hajdu[1], P. Hidas, D. Horvath[15], A. Kapusi, K. Krajczar[16], F. Sikler[1], G. Vesztergombi[16]

Institute of Nuclear Research ATOMKI, Debrecen, Hungary
N. Beni, J. Molnar, J. Palinkas, Z. Szillasi, V. Veszpremi

University of Debrecen, Debrecen, Hungary
J. Karancsi, P. Raics, Z.L. Trocsanyi, B. Ujvari

Panjab University, Chandigarh, India
S.B. Beri, V. Bhatnagar, N. Dhingra, R. Gupta, M. Jindal, M. Kaur, J.M. Kohli, M.Z. Mehta, N. Nishu, L.K. Saini, A. Sharma, A.P. Singh, J. Singh, S.P. Singh

University of Delhi, Delhi, India
S. Ahuja, B.C. Choudhary, A. Kumar, A. Kumar, S. Malhotra, M. Naimuddin, K. Ranjan, V. Sharma, R.K. Shivpuri

Saha Institute of Nuclear Physics, Kolkata, India
S. Banerjee, S. Bhattacharya, S. Dutta, B. Gomber, S. Jain, S. Jain, R. Khurana, S. Sarkar

Bhabha Atomic Research Centre, Mumbai, India
R.K. Choudhury, D. Dutta, S. Kailas, V. Kumar, A.K. Mohanty[1], L.M. Pant, P. Shukla

Tata Institute of Fundamental Research - EHEP, Mumbai, India
T. Aziz, S. Ganguly, M. Guchait[17], A. Gurtu, M. Maity[18], D. Majumder, G. Majumder, K. Mazumdar, G.B. Mohanty, B. Parida, A. Saha, K. Sudhakar, N. Wickramage

Tata Institute of Fundamental Research - HECR, Mumbai, India
S. Banerjee, S. Dugad, N.K. Mondal

Institute for Research and Fundamental Sciences (IPM), Tehran, Iran
H. Arfaei, H. Bakhshiansohi[19], S.M. Etesami[20], A. Fahim[19], M. Hashemi, H. Hesari, A. Jafari[19], M. Khakzad, A. Mohammadi[21], M. Mohammadi Najafabadi, S. Paktinat Mehdiabadi, B. Safarzadeh, M. Zeinali[20]

INFN Sezione di Bari [a], Università di Bari [b], Politecnico di Bari [c], Bari, Italy
M. Abbrescia[a,b], L. Barbone[a,b], C. Calabria[a,b], A. Colaleo[a], D. Creanza[a,c], N. De Filippis[a,c,1], M. De Palma[a,b], L. Fiore[a], G. Iaselli[a,c], L. Lusito[a,b], G. Maggi[a,c], M. Maggi[a], N. Manna[a,b], B. Marangelli[a,b], S. My[a,c], S. Nuzzo[a,b], N. Pacifico[a,b], A. Pompili[a,b], G. Pugliese[a,c], F. Romano[a,c], G. Selvaggi[a,b], L. Silvestris[a], S. Tupputi[a,b], G. Zito[a]

INFN Sezione di Bologna [a], Università di Bologna [b], Bologna, Italy
G. Abbiendi[a], A.C. Benvenuti[a], D. Bonacorsi[a], S. Braibant-Giacomelli[a,b], L. Brigliadori[a], P. Capiluppi[a,b], A. Castro[a,b], F.R. Cavallo[a], M. Cuffiani[a,b], G.M. Dallavalle[a], F. Fabbri[a], A. Fanfani[a,b], D. Fasanella[a,1], P. Giacomelli[a], C. Grandi[a], S. Marcellini[a], G. Masetti[a], M. Meneghelli[a,b], A. Montanari[a], F.L. Navarria[a,b], F. Odorici[a], A. Perrotta[a], F. Primavera[a], A.M. Rossi[a,b], T. Rovelli[a,b], G. Siroli[a,b], R. Travaglini[a,b]

INFN Sezione di Catania [a], Università di Catania [b], Catania, Italy
S. Albergo[a,b], G. Cappello[a,b], M. Chiorboli[a,b], S. Costa[a,b], R. Potenza[a,b], A. Tricomi[a,b], C. Tuve[a,b]

INFN Sezione di Firenze [a], Università di Firenze [b], Firenze, Italy
G. Barbagli[a], V. Ciulli[a,b], C. Civinini[a], R. D'Alessandro[a,b], E. Focardi[a,b], S. Frosali[a,b], E. Gallo[a], S. Gonzi[a,b], M. Meschini[a], S. Paoletti[a], G. Sguazzoni[a], A. Tropiano[a,1]

INFN Laboratori Nazionali di Frascati, Frascati, Italy
L. Benussi, S. Bianco, S. Colafranceschi[22], F. Fabbri, D. Piccolo

INFN Sezione di Genova, Genova, Italy
P. Fabbricatore, R. Musenich

INFN Sezione di Milano-Bicocca [a], Università di Milano-Bicocca [b], Milano, Italy
A. Benaglia[a,b,1], F. De Guio[a,b], L. Di Matteo[a,b], S. Gennai[a,1], A. Ghezzi[a,b], S. Malvezzi[a], A. Martelli[a,b], A. Massironi[a,b,1], D. Menasce[a], L. Moroni[a], M. Paganoni[a,b], D. Pedrini[a], S. Ragazzi[a,b], N. Redaelli[a], S. Sala[a], T. Tabarelli de Fatis[a,b]

INFN Sezione di Napoli [a], Università di Napoli "Federico II" [b], Napoli, Italy
S. Buontempo[a], C.A. Carrillo Montoya[a,1], N. Cavallo[a,23], A. De Cosa[a,b], O. Dogangun[a,b], F. Fabozzi[a,23], A.O.M. Iorio[a,1], L. Lista[a], M. Merola[a,b], P. Paolucci[a]

INFN Sezione di Padova [a], Università di Padova [b], Università di Trento (Trento) [c], Padova, Italy
P. Azzi[a], N. Bacchetta[a,1], P. Bellan[a,b], D. Bisello[a,b], A. Branca[a], R. Carlin[a,b], P. Checchia[a], T. Dorigo[a], U. Dosselli[a], F. Fanzago[a], F. Gasparini[a,b], U. Gasparini[a,b], A. Gozzelino[a], S. Lacaprara[a,24], I. Lazzizzera[a,c], M. Margoni[a,b], M. Mazzucato[a], A.T. Meneguzzo[a,b], M. Nespolo[a,1], L. Perrozzi[a], N. Pozzobon[a,b], P. Ronchese[a,b], F. Simonetto[a,b], E. Torassa[a], M. Tosi[a,b,1], S. Vanini[a,b], P. Zotto[a,b], G. Zumerle[a,b]

INFN Sezione di Pavia [a], Università di Pavia [b], Pavia, Italy
P. Baesso[a,b], U. Berzano[a], S.P. Ratti[a,b], C. Riccardi[a,b], P. Torre[a,b], P. Vitulo[a,b], C. Viviani[a,b]

INFN Sezione di Perugia [a], Università di Perugia [b], Perugia, Italy
M. Biasini[a,b], G.M. Bilei[a], B. Caponeri[a,b], L. Fanò[a,b], P. Lariccia[a,b], A. Lucaroni[a,b,1], G. Mantovani[a,b], M. Menichelli[a], A. Nappi[a,b], F. Romeo[a,b], A. Santocchia[a,b], S. Taroni[a,b,1], M. Valdata[a,b]

INFN Sezione di Pisa [a], Università di Pisa [b], Scuola Normale Superiore di Pisa [c], Pisa, Italy
P. Azzurri[a,c], G. Bagliesi[a], T. Boccali[a], G. Broccolo[a,c], R. Castaldi[a], R.T. D'Agnolo[a,c], R. Dell'Orso[a], F. Fiori[a,b], L. Foà[a,c], A. Giassi[a], A. Kraan[a], F. Ligabue[a,c], T. Lomtadze[a],

L. Martini[a,25], A. Messineo[a,b], F. Palla[a], F. Palmonari[a], A. Rizzi, G. Segneri[a], A.T. Serban[a], P. Spagnolo[a], R. Tenchini[a], G. Tonelli[a,b,1], A. Venturi[a,1], P.G. Verdini[a]

INFN Sezione di Roma [a], Università di Roma "La Sapienza" [b], Roma, Italy
L. Barone[a,b], F. Cavallari[a], D. Del Re[a,b,1], M. Diemoz[a], D. Franci[a,b], M. Grassi[a,1], E. Longo[a,b], P. Meridiani[a], S. Nourbakhsh[a], G. Organtini[a,b], F. Pandolfi[a,b], R. Paramatti[a], S. Rahatlou[a,b], M. Sigamani[a]

INFN Sezione di Torino [a], Università di Torino [b], Università del Piemonte Orientale (Novara) [c], Torino, Italy
N. Amapane[a,b], R. Arcidiacono[a,c], S. Argiro[a,b], M. Arneodo[a,c], C. Biino[a], C. Botta[a,b], N. Cartiglia[a], R. Castello[a,b], M. Costa[a,b], N. Demaria[a], A. Graziano[a,b], C. Mariotti[a,1], S. Maselli[a], E. Migliore[a,b], V. Monaco[a,b], M. Musich[a], M.M. Obertino[a,c], N. Pastrone[a], M. Pelliccioni[a], A. Potenza[a,b], A. Romero[a,b], M. Ruspa[a,c], R. Sacchi[a,b], V. Sola[a,b], A. Solano[a,b], A. Staiano[a], A. Vilela Pereira[a]

INFN Sezione di Trieste [a], Università di Trieste [b], Trieste, Italy
S. Belforte[a], F. Cossutti[a], G. Della Ricca[a,b], B. Gobbo[a], M. Marone[a,b], D. Montanino[a,b,1], A. Penzo[a]

Kangwon National University, Chunchon, Korea
S.G. Heo, S.K. Nam

Kyungpook National University, Daegu, Korea
S. Chang, J. Chung, D.H. Kim, G.N. Kim, J.E. Kim, D.J. Kong, H. Park, S.R. Ro, D.C. Son, T. Son

Chonnam National University, Institute for Universe and Elementary Particles, Kwangju, Korea
J.Y. Kim, Zero J. Kim, S. Song

Konkuk University, Seoul, Korea
H.Y. Jo

Korea University, Seoul, Korea
S. Choi, D. Gyun, B. Hong, M. Jo, H. Kim, T.J. Kim, K.S. Lee, D.H. Moon, S.K. Park, E. Seo, K.S. Sim

University of Seoul, Seoul, Korea
M. Choi, S. Kang, H. Kim, J.H. Kim, C. Park, I.C. Park, S. Park, G. Ryu

Sungkyunkwan University, Suwon, Korea
Y. Cho, Y. Choi, Y.K. Choi, J. Goh, M.S. Kim, B. Lee, J. Lee, S. Lee, H. Seo, I. Yu

Vilnius University, Vilnius, Lithuania
M.J. Bilinskas, I. Grigelionis, M. Janulis, D. Martisiute, P. Petrov, M. Polujanskas, T. Sabonis

Centro de Investigacion y de Estudios Avanzados del IPN, Mexico City, Mexico
H. Castilla-Valdez, E. De La Cruz-Burelo, I. Heredia-de La Cruz, R. Lopez-Fernandez, R. Magaña Villalba, J. Martínez-Ortega, A. Sánchez-Hernández, L.M. Villasenor-Cendejas

Universidad Iberoamericana, Mexico City, Mexico
S. Carrillo Moreno, F. Vazquez Valencia

Benemerita Universidad Autonoma de Puebla, Puebla, Mexico
H.A. Salazar Ibarguen

Universidad Autónoma de San Luis Potosí, San Luis Potosí, Mexico
E. Casimiro Linares, A. Morelos Pineda, M.A. Reyes-Santos

University of Auckland, Auckland, New Zealand
D. Krofcheck

University of Canterbury, Christchurch, New Zealand
A.J. Bell, P.H. Butler, R. Doesburg, S. Reucroft, H. Silverwood, N. Tambe

National Centre for Physics, Quaid-I-Azam University, Islamabad, Pakistan
M. Ahmad, M.I. Asghar, H.R. Hoorani, S. Khalid, W.A. Khan, T. Khurshid, S. Qazi, M.A. Shah, M. Shoaib

Institute of Experimental Physics, Faculty of Physics, University of Warsaw, Warsaw, Poland
G. Brona, M. Cwiok, W. Dominik, K. Doroba, A. Kalinowski, M. Konecki, J. Krolikowski

Soltan Institute for Nuclear Studies, Warsaw, Poland
H. Bialkowska, B. Boimska, T. Frueboes, R. Gokieli, M. Górski, M. Kazana, K. Nawrocki, K. Romanowska-Rybinska, M. Szleper, G. Wrochna, P. Zalewski

Laboratório de Instrumentação e Física Experimental de Partículas, Lisboa, Portugal
N. Almeida, P. Bargassa, A. David, P. Faccioli, P.G. Ferreira Parracho, M. Gallinaro, P. Musella, A. Nayak, J. Pela[1], P.Q. Ribeiro, J. Seixas, J. Varela

Joint Institute for Nuclear Research, Dubna, Russia
S. Afanasiev, I. Belotelov, P. Bunin, M. Gavrilenko, I. Golutvin, I. Gorbunov, A. Kamenev, V. Karjavin, G. Kozlov, A. Lanev, P. Moisenz, V. Palichik, V. Perelygin, S. Shmatov, V. Smirnov, A. Volodko, A. Zarubin

Petersburg Nuclear Physics Institute, Gatchina (St Petersburg), Russia
S. Evstyukhin, V. Golovtsov, Y. Ivanov, V. Kim, P. Levchenko, V. Murzin, V. Oreshkin, I. Smirnov, V. Sulimov, L. Uvarov, S. Vavilov, A. Vorobyev, An. Vorobyev

Institute for Nuclear Research, Moscow, Russia
Yu. Andreev, A. Dermenev, S. Gninenko, N. Golubev, M. Kirsanov, N. Krasnikov, V. Matveev, A. Pashenkov, A. Toropin, S. Troitsky

Institute for Theoretical and Experimental Physics, Moscow, Russia
V. Epshteyn, M. Erofeeva, V. Gavrilov, M. Kossov[1], A. Krokhotin, N. Lychkovskaya, V. Popov, G. Safronov, S. Semenov, V. Stolin, E. Vlasov, A. Zhokin

Moscow State University, Moscow, Russia
A. Belyaev, E. Boos, M. Dubinin[4], L. Dudko, A. Ershov, A. Gribushin, O. Kodolova, I. Lokhtin, A. Markina, S. Obraztsov, M. Perfilov, S. Petrushanko, L. Sarycheva, V. Savrin, A. Snigirev

P.N. Lebedev Physical Institute, Moscow, Russia
V. Andreev, M. Azarkin, I. Dremin, M. Kirakosyan, A. Leonidov, G. Mesyats, S.V. Rusakov, A. Vinogradov

State Research Center of Russian Federation, Institute for High Energy Physics, Protvino, Russia
I. Azhgirey, I. Bayshev, S. Bitioukov, V. Grishin[1], V. Kachanov, D. Konstantinov, A. Korablev, V. Krychkine, V. Petrov, R. Ryutin, A. Sobol, L. Tourtchanovitch, S. Troshin, N. Tyurin, A. Uzunian, A. Volkov

University of Belgrade, Faculty of Physics and Vinca Institute of Nuclear Sciences, Belgrade, Serbia
P. Adzic[26], M. Djordjevic, M. Ekmedzic, D. Krpic[26], J. Milosevic

Centro de Investigaciones Energéticas Medioambientales y Tecnológicas (CIEMAT), Madrid, Spain
M. Aguilar-Benitez, J. Alcaraz Maestre, P. Arce, C. Battilana, E. Calvo, M. Cerrada, M. Chamizo Llatas, N. Colino, B. De La Cruz, A. Delgado Peris, C. Diez Pardos, D. Domínguez Vázquez, C. Fernandez Bedoya, J.P. Fernández Ramos, A. Ferrando, J. Flix, M.C. Fouz, P. Garcia-Abia, O. Gonzalez Lopez, S. Goy Lopez, J.M. Hernandez, M.I. Josa, G. Merino, J. Puerta Pelayo, I. Redondo, L. Romero, J. Santaolalla, M.S. Soares, C. Willmott

Universidad Autónoma de Madrid, Madrid, Spain
C. Albajar, G. Codispoti, J.F. de Trocóniz

Universidad de Oviedo, Oviedo, Spain
J. Cuevas, J. Fernandez Menendez, S. Folgueras, I. Gonzalez Caballero, L. Lloret Iglesias, J.M. Vizan Garcia

Instituto de Física de Cantabria (IFCA), CSIC-Universidad de Cantabria, Santander, Spain
J.A. Brochero Cifuentes, I.J. Cabrillo, A. Calderon, S.H. Chuang, J. Duarte Campderros, M. Felcini[27], M. Fernandez, G. Gomez, J. Gonzalez Sanchez, C. Jorda, P. Lobelle Pardo, A. Lopez Virto, J. Marco, R. Marco, C. Martinez Rivero, F. Matorras, F.J. Munoz Sanchez, J. Piedra Gomez[28], T. Rodrigo, A.Y. Rodríguez-Marrero, A. Ruiz-Jimeno, L. Scodellaro, M. Sobron Sanudo, I. Vila, R. Vilar Cortabitarte

CERN, European Organization for Nuclear Research, Geneva, Switzerland
D. Abbaneo, E. Auffray, G. Auzinger, P. Baillon, A.H. Ball, D. Barney, C. Bernet[5], W. Bialas, P. Bloch, A. Bocci, H. Breuker, K. Bunkowski, T. Camporesi, G. Cerminara, T. Christiansen, J.A. Coarasa Perez, B. Curé, D. D'Enterria, A. De Roeck, S. Di Guida, M. Dobson, N. Dupont-Sagorin, A. Elliott-Peisert, B. Frisch, W. Funk, A. Gaddi, G. Georgiou, H. Gerwig, M. Giffels, D. Gigi, K. Gill, D. Giordano, M. Giunta, F. Glege, R. Gomez-Reino Garrido, P. Govoni, S. Gowdy, R. Guida, L. Guiducci, S. Gundacker, M. Hansen, C. Hartl, J. Harvey, J. Hegeman, B. Hegner, A. Hinzmann, H.F. Hoffmann, V. Innocente, P. Janot, K. Kaadze, E. Karavakis, K. Kousouris, P. Lecoq, P. Lenzi, C. Lourenço, T. Mäki, M. Malberti, L. Malgeri, M. Mannelli, L. Masetti, G. Mavromanolakis, F. Meijers, S. Mersi, E. Meschi, R. Moser, M.U. Mozer, M. Mulders, E. Nesvold, M. Nguyen, T. Orimoto, L. Orsini, E. Palencia Cortezon, E. Perez, A. Petrilli, A. Pfeiffer, M. Pierini, M. Pimiä, D. Piparo, G. Polese, L. Quertenmont, A. Racz, W. Reece, J. Rodrigues Antunes, G. Rolandi[29], T. Rommerskirchen, C. Rovelli[30], M. Rovere, H. Sakulin, F. Santanastasio, C. Schäfer, C. Schwick, I. Segoni, A. Sharma, P. Siegrist, P. Silva, M. Simon, P. Sphicas[31], D. Spiga, M. Spiropulu[4], M. Stoye, A. Tsirou, G.I. Veres[16], P. Vichoudis, H.K. Wöhri, S.D. Worm[32], W.D. Zeuner

Paul Scherrer Institut, Villigen, Switzerland
W. Bertl, K. Deiters, W. Erdmann, K. Gabathuler, R. Horisberger, Q. Ingram, H.C. Kaestli, S. König, D. Kotlinski, U. Langenegger, F. Meier, D. Renker, T. Rohe, J. Sibille[33]

Institute for Particle Physics, ETH Zurich, Zurich, Switzerland
L. Bäni, P. Bortignon, M.A. Buchmann, B. Casal, N. Chanon, Z. Chen, S. Cittolin, A. Deisher, G. Dissertori, M. Dittmar, J. Eugster, K. Freudenreich, C. Grab, P. Lecomte, W. Lustermann, P. Martinez Ruiz del Arbol, P. Milenovic[34], N. Mohr, F. Moortgat, C. Nägeli[35], P. Nef, F. Nessi-Tedaldi, L. Pape, F. Pauss, M. Peruzzi, F.J. Ronga, M. Rossini, L. Sala, A.K. Sanchez, M.-

C. Sawley, A. Starodumov[36], B. Stieger, M. Takahashi, L. Tauscher[†], A. Thea, K. Theofilatos, D. Treille, C. Urscheler, R. Wallny, H.A. Weber, L. Wehrli, J. Weng

Universität Zürich, Zurich, Switzerland
E. Aguilo, C. Amsler, V. Chiochia, S. De Visscher, C. Favaro, M. Ivova Rikova, B. Millan Mejias, P. Otiougova, P. Robmann, A. Schmidt, H. Snoek, M. Verzetti

National Central University, Chung-Li, Taiwan
Y.H. Chang, K.H. Chen, C.M. Kuo, S.W. Li, W. Lin, Z.K. Liu, Y.J. Lu, D. Mekterovic, R. Volpe, S.S. Yu

National Taiwan University (NTU), Taipei, Taiwan
P. Bartalini, P. Chang, Y.H. Chang, Y.W. Chang, Y. Chao, K.F. Chen, C. Dietz, U. Grundler, W.-S. Hou, Y. Hsiung, K.Y. Kao, Y.J. Lei, R.-S. Lu, J.G. Shiu, Y.M. Tzeng, X. Wan, M. Wang

Cukurova University, Adana, Turkey
A. Adiguzel, M.N. Bakirci[37], S. Cerci[38], C. Dozen, I. Dumanoglu, E. Eskut, S. Girgis, G. Gokbulut, I. Hos, E.E. Kangal, G. Karapinar, A. Kayis Topaksu, G. Onengut, K. Ozdemir, S. Ozturk[39], A. Polatoz, K. Sogut[40], D. Sunar Cerci[38], B. Tali[38], H. Topakli[37], D. Uzun, L.N. Vergili, M. Vergili

Middle East Technical University, Physics Department, Ankara, Turkey
I.V. Akin, T. Aliev, B. Bilin, S. Bilmis, M. Deniz, H. Gamsizkan, A.M. Guler, K. Ocalan, A. Ozpineci, M. Serin, R. Sever, U.E. Surat, M. Yalvac, E. Yildirim, M. Zeyrek

Bogazici University, Istanbul, Turkey
M. Deliomeroglu, E. Gülmez, B. Isildak, M. Kaya[41], O. Kaya[41], S. Ozkorucuklu[42], N. Sonmez[43]

National Scientific Center, Kharkov Institute of Physics and Technology, Kharkov, Ukraine
L. Levchuk

University of Bristol, Bristol, United Kingdom
F. Bostock, J.J. Brooke, E. Clement, D. Cussans, H. Flacher, R. Frazier, J. Goldstein, M. Grimes, G.P. Heath, H.F. Heath, L. Kreczko, S. Metson, D.M. Newbold[32], K. Nirunpong, A. Poll, S. Senkin, V.J. Smith, T. Williams

Rutherford Appleton Laboratory, Didcot, United Kingdom
L. Basso[44], K.W. Bell, A. Belyaev[44], C. Brew, R.M. Brown, B. Camanzi, D.J.A. Cockerill, J.A. Coughlan, K. Harder, S. Harper, J. Jackson, B.W. Kennedy, E. Olaiya, D. Petyt, B.C. Radburn-Smith, C.H. Shepherd-Themistocleous, I.R. Tomalin, W.J. Womersley

Imperial College, London, United Kingdom
R. Bainbridge, G. Ball, R. Beuselinck, O. Buchmuller, D. Colling, N. Cripps, M. Cutajar, P. Dauncey, G. Davies, M. Della Negra, W. Ferguson, J. Fulcher, D. Futyan, A. Gilbert, A. Guneratne Bryer, G. Hall, Z. Hatherell, J. Hays, G. Iles, M. Jarvis, G. Karapostoli, L. Lyons, A.-M. Magnan, J. Marrouche, B. Mathias, R. Nandi, J. Nash, A. Nikitenko[36], A. Papageorgiou, M. Pesaresi, K. Petridis, M. Pioppi[45], D.M. Raymond, S. Rogerson, N. Rompotis, A. Rose, M.J. Ryan, C. Seez, P. Sharp, A. Sparrow, A. Tapper, S. Tourneur, M. Vazquez Acosta, T. Virdee, S. Wakefield, N. Wardle, D. Wardrope, T. Whyntie

Brunel University, Uxbridge, United Kingdom
M. Barrett, M. Chadwick, J.E. Cole, P.R. Hobson, A. Khan, P. Kyberd, D. Leslie, W. Martin, I.D. Reid, P. Symonds, L. Teodorescu, M. Turner

Baylor University, Waco, USA
K. Hatakeyama, H. Liu, T. Scarborough

The University of Alabama, Tuscaloosa, USA
C. Henderson

Boston University, Boston, USA
A. Avetisyan, T. Bose, E. Carrera Jarrin, C. Fantasia, A. Heister, J. St. John, P. Lawson, D. Lazic, J. Rohlf, D. Sperka, L. Sulak

Brown University, Providence, USA
S. Bhattacharya, D. Cutts, A. Ferapontov, U. Heintz, S. Jabeen, G. Kukartsev, G. Landsberg, M. Luk, M. Narain, D. Nguyen, M. Segala, T. Sinthuprasith, T. Speer, K.V. Tsang

University of California, Davis, Davis, USA
R. Breedon, G. Breto, M. Calderon De La Barca Sanchez, S. Chauhan, M. Chertok, J. Conway, R. Conway, P.T. Cox, J. Dolen, R. Erbacher, R. Houtz, W. Ko, A. Kopecky, R. Lander, O. Mall, T. Miceli, D. Pellett, J. Robles, B. Rutherford, M. Searle, J. Smith, M. Squires, M. Tripathi, R. Vasquez Sierra

University of California, Los Angeles, Los Angeles, USA
V. Andreev, K. Arisaka, D. Cline, R. Cousins, J. Duris, S. Erhan, P. Everaerts, C. Farrell, J. Hauser, M. Ignatenko, C. Jarvis, C. Plager, G. Rakness, P. Schlein[†], J. Tucker, V. Valuev, M. Weber

University of California, Riverside, Riverside, USA
J. Babb, R. Clare, J. Ellison, J.W. Gary, F. Giordano, G. Hanson, G.Y. Jeng, H. Liu, O.R. Long, A. Luthra, H. Nguyen, S. Paramesvaran, J. Sturdy, S. Sumowidagdo, R. Wilken, S. Wimpenny

University of California, San Diego, La Jolla, USA
W. Andrews, J.G. Branson, G.B. Cerati, D. Evans, F. Golf, A. Holzner, R. Kelley, M. Lebourgeois, J. Letts, I. Macneill, B. Mangano, S. Padhi, C. Palmer, G. Petrucciani, H. Pi, M. Pieri, R. Ranieri, M. Sani, I. Sfiligoi, V. Sharma, S. Simon, E. Sudano, M. Tadel, Y. Tu, A. Vartak, S. Wasserbaech[46], F. Würthwein, A. Yagil, J. Yoo

University of California, Santa Barbara, Santa Barbara, USA
D. Barge, R. Bellan, C. Campagnari, M. D'Alfonso, T. Danielson, K. Flowers, P. Geffert, C. George, J. Incandela, C. Justus, P. Kalavase, S.A. Koay, D. Kovalskyi[1], V. Krutelyov, S. Lowette, N. Mccoll, S.D. Mullin, V. Pavlunin, F. Rebassoo, J. Ribnik, J. Richman, R. Rossin, D. Stuart, W. To, J.R. Vlimant, C. West

California Institute of Technology, Pasadena, USA
A. Apresyan, A. Bornheim, J. Bunn, Y. Chen, E. Di Marco, J. Duarte, M. Gataullin, Y. Ma, A. Mott, H.B. Newman, C. Rogan, V. Timciuc, P. Traczyk, J. Veverka, R. Wilkinson, Y. Yang, R.Y. Zhu

Carnegie Mellon University, Pittsburgh, USA
B. Akgun, R. Carroll, T. Ferguson, Y. Iiyama, D.W. Jang, S.Y. Jun, Y.F. Liu, M. Paulini, J. Russ, H. Vogel, I. Vorobiev

University of Colorado at Boulder, Boulder, USA
J.P. Cumalat, M.E. Dinardo, B.R. Drell, C.J. Edelmaier, W.T. Ford, A. Gaz, B. Heyburn, E. Luiggi Lopez, U. Nauenberg, J.G. Smith, K. Stenson, K.A. Ulmer, S.R. Wagner, S.L. Zang

Cornell University, Ithaca, USA
L. Agostino, J. Alexander, A. Chatterjee, N. Eggert, L.K. Gibbons, B. Heltsley, W. Hopkins,

A. Khukhunaishvili, B. Kreis, G. Nicolas Kaufman, J.R. Patterson, D. Puigh, A. Ryd, E. Salvati, X. Shi, W. Sun, W.D. Teo, J. Thom, J. Thompson, J. Vaughan, Y. Weng, L. Winstrom, P. Wittich

Fairfield University, Fairfield, USA
A. Biselli, G. Cirino, D. Winn

Fermi National Accelerator Laboratory, Batavia, USA
S. Abdullin, M. Albrow, J. Anderson, G. Apollinari, M. Atac, J.A. Bakken, L.A.T. Bauerdick, A. Beretvas, J. Berryhill, P.C. Bhat, I. Bloch, K. Burkett, J.N. Butler, V. Chetluru, H.W.K. Cheung, F. Chlebana, S. Cihangir, W. Cooper, D.P. Eartly, V.D. Elvira, S. Esen, I. Fisk, J. Freeman, Y. Gao, E. Gottschalk, D. Green, O. Gutsche, J. Hanlon, R.M. Harris, J. Hirschauer, B. Hooberman, H. Jensen, S. Jindariani, M. Johnson, U. Joshi, B. Klima, S. Kunori, S. Kwan, C. Leonidopoulos, D. Lincoln, R. Lipton, J. Lykken, K. Maeshima, J.M. Marraffino, S. Maruyama, D. Mason, P. McBride, T. Miao, K. Mishra, S. Mrenna, Y. Musienko[47], C. Newman-Holmes, V. O'Dell, J. Pivarski, R. Pordes, O. Prokofyev, T. Schwarz, E. Sexton-Kennedy, S. Sharma, W.J. Spalding, L. Spiegel, P. Tan, L. Taylor, S. Tkaczyk, L. Uplegger, E.W. Vaandering, R. Vidal, J. Whitmore, W. Wu, F. Yang, F. Yumiceva, J.C. Yun

University of Florida, Gainesville, USA
D. Acosta, P. Avery, D. Bourilkov, M. Chen, S. Das, M. De Gruttola, G.P. Di Giovanni, D. Dobur, A. Drozdetskiy, R.D. Field, M. Fisher, Y. Fu, I.K. Furic, J. Gartner, S. Goldberg, J. Hugon, B. Kim, J. Konigsberg, A. Korytov, A. Kropivnitskaya, T. Kypreos, J.F. Low, K. Matchev, G. Mitselmakher, L. Muniz, P. Myeonghun, R. Remington, A. Rinkevicius, M. Schmitt, B. Scurlock, P. Sellers, N. Skhirtladze, M. Snowball, D. Wang, J. Yelton, M. Zakaria

Florida International University, Miami, USA
V. Gaultney, L.M. Lebolo, S. Linn, P. Markowitz, G. Martinez, J.L. Rodriguez

Florida State University, Tallahassee, USA
T. Adams, A. Askew, J. Bochenek, J. Chen, B. Diamond, S.V. Gleyzer, J. Haas, S. Hagopian, V. Hagopian, M. Jenkins, K.F. Johnson, H. Prosper, S. Sekmen, V. Veeraraghavan, M. Weinberg

Florida Institute of Technology, Melbourne, USA
M.M. Baarmand, B. Dorney, M. Hohlmann, H. Kalakhety, I. Vodopiyanov

University of Illinois at Chicago (UIC), Chicago, USA
M.R. Adams, I.M. Anghel, L. Apanasevich, Y. Bai, V.E. Bazterra, R.R. Betts, J. Callner, R. Cavanaugh, C. Dragoiu, L. Gauthier, C.E. Gerber, D.J. Hofman, S. Khalatyan, G.J. Kunde[48], F. Lacroix, M. Malek, C. O'Brien, C. Silkworth, C. Silvestre, D. Strom, N. Varelas

The University of Iowa, Iowa City, USA
U. Akgun, E.A. Albayrak, B. Bilki, W. Clarida, F. Duru, S. Griffiths, C.K. Lae, E. McCliment, J.-P. Merlo, H. Mermerkaya[49], A. Mestvirishvili, A. Moeller, J. Nachtman, C.R. Newsom, E. Norbeck, J. Olson, Y. Onel, F. Ozok, S. Sen, E. Tiras, J. Wetzel, T. Yetkin, K. Yi

Johns Hopkins University, Baltimore, USA
B.A. Barnett, B. Blumenfeld, S. Bolognesi, A. Bonato, C. Eskew, D. Fehling, G. Giurgiu, A.V. Gritsan, Z.J. Guo, G. Hu, P. Maksimovic, S. Rappoccio, M. Swartz, N.V. Tran, A. Whitbeck

The University of Kansas, Lawrence, USA
P. Baringer, A. Bean, G. Benelli, O. Grachov, R.P. Kenny Iii, M. Murray, D. Noonan, S. Sanders, R. Stringer, G. Tinti, J.S. Wood, V. Zhukova

Kansas State University, Manhattan, USA
A.F. Barfuss, T. Bolton, I. Chakaberia, A. Ivanov, S. Khalil, M. Makouski, Y. Maravin, S. Shrestha, I. Svintradze

Lawrence Livermore National Laboratory, Livermore, USA
J. Gronberg, D. Lange, D. Wright

University of Maryland, College Park, USA
A. Baden, M. Boutemeur, B. Calvert, S.C. Eno, J.A. Gomez, N.J. Hadley, R.G. Kellogg, M. Kirn, T. Kolberg, Y. Lu, A.C. Mignerey, A. Peterman, K. Rossato, P. Rumerio, A. Skuja, J. Temple, M.B. Tonjes, S.C. Tonwar, E. Twedt

Massachusetts Institute of Technology, Cambridge, USA
B. Alver, G. Bauer, J. Bendavid, W. Busza, E. Butz, I.A. Cali, M. Chan, V. Dutta, G. Gomez Ceballos, M. Goncharov, K.A. Hahn, P. Harris, Y. Kim, M. Klute, Y.-J. Lee, W. Li, P.D. Luckey, T. Ma, S. Nahn, C. Paus, D. Ralph, C. Roland, G. Roland, M. Rudolph, G.S.F. Stephans, F. Stöckli, K. Sumorok, K. Sung, D. Velicanu, E.A. Wenger, R. Wolf, B. Wyslouch, S. Xie, M. Yang, Y. Yilmaz, A.S. Yoon, M. Zanetti

University of Minnesota, Minneapolis, USA
S.I. Cooper, P. Cushman, B. Dahmes, A. De Benedetti, G. Franzoni, A. Gude, J. Haupt, S.C. Kao, K. Klapoetke, Y. Kubota, J. Mans, N. Pastika, V. Rekovic, R. Rusack, M. Sasseville, A. Singovsky, J. Turkewitz

University of Mississippi, University, USA
L.M. Cremaldi, R. Godang, R. Kroeger, L. Perera, R. Rahmat, D.A. Sanders, D. Summers

University of Nebraska-Lincoln, Lincoln, USA
E. Avdeeva, K. Bloom, S. Bose, J. Butt, D.R. Claes, A. Dominguez, M. Eads, P. Jindal, J. Keller, I. Kravchenko, J. Lazo-Flores, H. Malbouisson, S. Malik, G.R. Snow

State University of New York at Buffalo, Buffalo, USA
U. Baur, A. Godshalk, I. Iashvili, S. Jain, A. Kharchilava, A. Kumar, S.P. Shipkowski, K. Smith, Z. Wan

Northeastern University, Boston, USA
G. Alverson, E. Barberis, D. Baumgartel, M. Chasco, D. Trocino, D. Wood, J. Zhang

Northwestern University, Evanston, USA
A. Anastassov, A. Kubik, N. Mucia, N. Odell, R.A. Ofierzynski, B. Pollack, A. Pozdnyakov, M. Schmitt, S. Stoynev, M. Velasco, S. Won

University of Notre Dame, Notre Dame, USA
L. Antonelli, D. Berry, A. Brinkerhoff, M. Hildreth, C. Jessop, D.J. Karmgard, J. Kolb, K. Lannon, W. Luo, S. Lynch, N. Marinelli, D.M. Morse, T. Pearson, R. Ruchti, J. Slaunwhite, N. Valls, M. Wayne, M. Wolf, J. Ziegler

The Ohio State University, Columbus, USA
B. Bylsma, L.S. Durkin, C. Hill, P. Killewald, K. Kotov, T.Y. Ling, M. Rodenburg, C. Vuosalo, G. Williams

Princeton University, Princeton, USA
N. Adam, E. Berry, P. Elmer, D. Gerbaudo, V. Halyo, P. Hebda, A. Hunt, E. Laird, D. Lopes Pegna, P. Lujan, D. Marlow, T. Medvedeva, M. Mooney, J. Olsen, P. Piroué, X. Quan, A. Raval, H. Saka, D. Stickland, C. Tully, J.S. Werner, A. Zuranski

University of Puerto Rico, Mayaguez, USA
J.G. Acosta, X.T. Huang, A. Lopez, H. Mendez, S. Oliveros, J.E. Ramirez Vargas, A. Zatserklyaniy

Purdue University, West Lafayette, USA
E. Alagoz, V.E. Barnes, D. Benedetti, G. Bolla, L. Borrello, D. Bortoletto, M. De Mattia, A. Everett, L. Gutay, Z. Hu, M. Jones, O. Koybasi, M. Kress, A.T. Laasanen, N. Leonardo, V. Maroussov, P. Merkel, D.H. Miller, N. Neumeister, I. Shipsey, D. Silvers, A. Svyatkovskiy, M. Vidal Marono, H.D. Yoo, J. Zablocki, Y. Zheng

Purdue University Calumet, Hammond, USA
S. Guragain, N. Parashar

Rice University, Houston, USA
A. Adair, C. Boulahouache, V. Cuplov, K.M. Ecklund, F.J.M. Geurts, B.P. Padley, R. Redjimi, J. Roberts, J. Zabel

University of Rochester, Rochester, USA
B. Betchart, A. Bodek, Y.S. Chung, R. Covarelli, P. de Barbaro, R. Demina, Y. Eshaq, A. Garcia-Bellido, P. Goldenzweig, Y. Gotra, J. Han, A. Harel, D.C. Miner, G. Petrillo, W. Sakumoto, D. Vishnevskiy, M. Zielinski

The Rockefeller University, New York, USA
A. Bhatti, R. Ciesielski, L. Demortier, K. Goulianos, G. Lungu, S. Malik, C. Mesropian

Rutgers, the State University of New Jersey, Piscataway, USA
S. Arora, O. Atramentov, A. Barker, J.P. Chou, C. Contreras-Campana, E. Contreras-Campana, D. Duggan, D. Ferencek, Y. Gershtein, R. Gray, E. Halkiadakis, D. Hidas, D. Hits, A. Lath, S. Panwalkar, M. Park, R. Patel, A. Richards, K. Rose, S. Salur, S. Schnetzer, S. Somalwar, R. Stone, S. Thomas

University of Tennessee, Knoxville, USA
G. Cerizza, M. Hollingsworth, S. Spanier, Z.C. Yang, A. York

Texas A&M University, College Station, USA
R. Eusebi, W. Flanagan, J. Gilmore, T. Kamon[50], V. Khotilovich, R. Montalvo, I. Osipenkov, Y. Pakhotin, A. Perloff, J. Roe, A. Safonov, S. Sengupta, I. Suarez, A. Tatarinov, D. Toback

Texas Tech University, Lubbock, USA
N. Akchurin, C. Bardak, J. Damgov, P.R. Dudero, C. Jeong, K. Kovitanggoon, S.W. Lee, T. Libeiro, P. Mane, Y. Roh, A. Sill, I. Volobouev, R. Wigmans, E. Yazgan

Vanderbilt University, Nashville, USA
E. Appelt, E. Brownson, D. Engh, C. Florez, W. Gabella, A. Gurrola, M. Issah, W. Johns, C. Johnston, P. Kurt, C. Maguire, A. Melo, P. Sheldon, B. Snook, S. Tuo, J. Velkovska

University of Virginia, Charlottesville, USA
M.W. Arenton, M. Balazs, S. Boutle, S. Conetti, B. Cox, B. Francis, S. Goadhouse, J. Goodell, R. Hirosky, A. Ledovskoy, C. Lin, C. Neu, J. Wood, R. Yohay

Wayne State University, Detroit, USA
S. Gollapinni, R. Harr, P.E. Karchin, C. Kottachchi Kankanamge Don, P. Lamichhane, M. Mattson, C. Milstène, A. Sakharov

University of Wisconsin, Madison, USA
M. Anderson, M. Bachtis, D. Belknap, J.N. Bellinger, J. Bernardini, D. Carlsmith, M. Cepeda,

S. Dasu, J. Efron, E. Friis, L. Gray, K.S. Grogg, M. Grothe, R. Hall-Wilton, M. Herndon, A. Hervé, P. Klabbers, J. Klukas, A. Lanaro, C. Lazaridis, J. Leonard, R. Loveless, A. Mohapatra, I. Ojalvo, G.A. Pierro, I. Ross, A. Savin, W.H. Smith, J. Swanson

†: Deceased
1: Also at CERN, European Organization for Nuclear Research, Geneva, Switzerland
2: Also at National Institute of Chemical Physics and Biophysics, Tallinn, Estonia
3: Also at Universidade Federal do ABC, Santo Andre, Brazil
4: Also at California Institute of Technology, Pasadena, USA
5: Also at Laboratoire Leprince-Ringuet, Ecole Polytechnique, IN2P3-CNRS, Palaiseau, France
6: Also at Suez Canal University, Suez, Egypt
7: Also at Cairo University, Cairo, Egypt
8: Also at British University, Cairo, Egypt
9: Also at Fayoum University, El-Fayoum, Egypt
10: Also at Ain Shams University, Cairo, Egypt
11: Also at Soltan Institute for Nuclear Studies, Warsaw, Poland
12: Also at Université de Haute-Alsace, Mulhouse, France
13: Also at Moscow State University, Moscow, Russia
14: Also at Brandenburg University of Technology, Cottbus, Germany
15: Also at Institute of Nuclear Research ATOMKI, Debrecen, Hungary
16: Also at Eötvös Loránd University, Budapest, Hungary
17: Also at Tata Institute of Fundamental Research - HECR, Mumbai, India
18: Also at University of Visva-Bharati, Santiniketan, India
19: Also at Sharif University of Technology, Tehran, Iran
20: Also at Isfahan University of Technology, Isfahan, Iran
21: Also at Shiraz University, Shiraz, Iran
22: Also at Facoltà Ingegneria Università di Roma, Roma, Italy
23: Also at Università della Basilicata, Potenza, Italy
24: Also at Laboratori Nazionali di Legnaro dell' INFN, Legnaro, Italy
25: Also at Università degli studi di Siena, Siena, Italy
26: Also at Faculty of Physics of University of Belgrade, Belgrade, Serbia
27: Also at University of California, Los Angeles, Los Angeles, USA
28: Also at University of Florida, Gainesville, USA
29: Also at Scuola Normale e Sezione dell' INFN, Pisa, Italy
30: Also at INFN Sezione di Roma; Università di Roma "La Sapienza", Roma, Italy
31: Also at University of Athens, Athens, Greece
32: Now at Rutherford Appleton Laboratory, Didcot, United Kingdom
33: Also at The University of Kansas, Lawrence, USA
34: Also at University of Belgrade, Faculty of Physics and Vinca Institute of Nuclear Sciences, Belgrade, Serbia
35: Also at Paul Scherrer Institut, Villigen, Switzerland
36: Also at Institute for Theoretical and Experimental Physics, Moscow, Russia
37: Also at Gaziosmanpasa University, Tokat, Turkey
38: Also at Adiyaman University, Adiyaman, Turkey
39: Also at The University of Iowa, Iowa City, USA
40: Also at Mersin University, Mersin, Turkey
41: Also at Kafkas University, Kars, Turkey
42: Also at Suleyman Demirel University, Isparta, Turkey
43: Also at Ege University, Izmir, Turkey
44: Also at School of Physics and Astronomy, University of Southampton, Southampton,

United Kingdom
45: Also at INFN Sezione di Perugia; Università di Perugia, Perugia, Italy
46: Also at Utah Valley University, Orem, USA
47: Also at Institute for Nuclear Research, Moscow, Russia
48: Also at Los Alamos National Laboratory, Los Alamos, USA
49: Also at Erzincan University, Erzincan, Turkey
50: Also at Kyungpook National University, Daegu, Korea